AN EXAMINATION INTO PHYSICAL CONTROLS

ON HYPORHEIC INTERCHANGE

Timothy B. Sickbert

48 Pages August 2005

An investigation into the potential of the *Venturi Effect* to affect hyporheic interchange, and a new *in situ* method for estimating hydraulic conductivity of streambed sediments.

APPROVED:

_____

Date Eric W. Peterson, Chair

_____

Date Steven J. Van der Hoven

_____

Date Dagmar Budikova

AN EXAMINATION INTO PHYSICAL CONTROLS ON HYPORHEIC INTERCHANGE

Timothy B. Sickbert

48 Pages August 2005

The *hyporheic zone* is the saturated space below surface water that connects surface and ground water into an integrated system. The mixing of the chemically distinct waters creates an oxygen- and nutrient-enriched environment, affecting the health of lotic and riparian ecosystems. The importance of the hyporheic zone has been recognized only recently, and difficulties remain in quantifying the surface-subsurface flux. This thesis explores the force—hydraulic head, h—that drives, and the stream bed characteristic—hydraulic conductivity, K—that restricts the exchange.

Water flows from a point of higher energy, or *total head*, to a point of lower energy. *Bernoulli's Equation* describes the energy in terms of static pressure, elevation, and velocity, the sum of which is constant. The *Venturi Effect* describes the consequence that as the velocity increases then pressure or elevation must decrease to maintain constancy of the total head. This is the effect by which airplanes derive lift. The first part of this thesis attempts to detect and measure the Venturi Effect resulting from differences in velocity as a stream rounds a meander.

While a difference in head drives flow, the stream bed material resists flow. The inverse of this resistance is the hydraulic conductivity, K. Many methods exist to

measure *K* in the laboratory and in subsurface aquifers, but these methods make assumptions that may not apply to the shallow subsurface of a stream bed. The second part of this thesis attempts to estimate *K* of streambed material *in situ* by calibrating a one-dimensional model to measured stage and logged shallow subsurface *h* data.

Neither part of this thesis met the objectives. In the first part, stream velocity did not vary sufficiently to create a Venturi Effect large enough to be detected by the instruments used. The results do, however, place an upper limit on the magnitude of the effect. In the second part, the model incorrectly assumed that head could substitute for mass in the model equation. Correcting this may lead to a refined model useful for estimating streambed *K*.

APPROVED:

_____

Date Eric W. Peterson, Chair

_____

Date Steven J. Van der Hoven

_____

Date Dagmar Budikova

AN EXAMINATION INTO PHYSICAL CONTROLS ON HYPORHEIC INTERCHANGE

TIMOTHY B. SICKBERT

A Thesis submitted in Partial
Fulfillment of the Requirements
for the Degree of

MASTER OF SCIENCE

Department of Geography-Geology

ILLINOIS STATE UNIVERSITY

2005

THESIS APPROVED:

Date Eric W. Peterson, Chair

Date Steven J. Van der Hoven

Date Dagmar Budikova

ACKNOWLEDGEMENTS

The writer wishes to thank the entire Department of Geography-Geology at Illinois State University for working so hard and so successfully to create a positive and encouraging, environment; Rebecca Sphar for her support and tolerance; and my parents for always challenging me intellectually while teaching me that good fun is hard work and that happiness is my choice.

The writer also wishes to acknowledge support from Oklahoma State University, from Sigma Xi, the Geological Society of America Graduate Research Award Program, and the Geological Society of America Quaternary Geology and Geomorphology Section, without whose support this work would not have been possible.

T. B. S.

CONTENTS

TABLES

FIGURES

CHAPTER I

AN EXAMINATION INTO THE PHYSICAL CONTROLS ON HYPORHEIC INTERCHANGE

Definition of the Hyporheic Zone

Historically, the study of water on and beneath the continental land surface has been divided into hydrology—the study of water sitting on the surface confined by beds and banks; and hydrogeology—the study of water beneath the surface (Boulton, 1998). This division is well-justified by the many differences between surface water and ground water. Surface water is frequently well-oxygenated, receives energy directly from insolation, may support diverse and abundant biota limited by availability of mineral nutrients, and resides in reservoirs for periods on the order of days to years before flowing to the oceans. Ground water is typically oxygen-poor, must rely on relict chemical energy derived from sediments or from primitive compounds, hosts only sparse fauna, carries an abundance of mineral nutrients, and may reside in the subsurface for periods ranging from decades to millennia. Although surface water and ground water are clearly distinct, in most instances where surface water exists, it continuously saturates the subsurface, hydraulically connecting the surface water with the ground water. Water may flow in either or both directions between the surface and subsurface reservouris. Near the surface, these waters mix and create an environment

enriched in both oxygen and mineral nutrients. This space is the *hyporheic zone*, or *hyporheos*.

Physical Controls on Hyporheic Flow

The flow of water on the surface, in the subsurface, and between the two is driven by a gradient in the fluid potential, and controlled by the ability of the material to conduct the flow. Significant components of total fluid potential include the pressure, elevation, and velocity of the water. In the subsurface, the velocity component of fluid potential is generally negligible and the term reduces to the sum of pressure and elevation, or *hydrostatic head* (*h)*. Within a flowing stream, the velocity component is significant where the water flows swiftly. Natural variations of streamflow velocity along and across the stream channel create local differences that can control the magnitude and direction of flux across the streambed surface. Thibideaux and Boyle (1987) experimentally demonstrated and mathematically described small-scale bedforms creating sufficient variability in *h* to drive flow into and draw flow from the streambed. Elliott and Brooks (1997a) developed an analytical model for the distribution of subsurface *h*, flux, and residence time under sinusoidally varying streambed surface *h*. Researchers have well established that bedform variability exerts a degree of physical control over flow into and out of the shallow stream bed, but the literature has focused on longitudinal variations. Similar dynamnic variability in *h* that occurs laterally across the stream channel has not been fully explored. In the presence of a gradient, the material through which the water flows resists the flow. The characteristic of a material describing its ability to transmit water is termed *hydraulic conductivity* (*K*), which is a

function of the size, sorting, and packing of the material. Stream channel beds and banks are typically sediments deposited by the stream under the full range of flow conditions. Therefore, the stream bed and bank material naturally varies over space and time at scales ranging from centimeters to tens of meters and minutes to centuries. The hyporheic zone is created and controlled by spatial and temporal variations in these parameters of *h* and *K* (Sophocleous, 2002).

Significance of the Hyporheic Zone

Hyporheic interchange is the small-scale (centimeters to hundreds of meters) flow of water between streams and the subsurface through the interstitial spaces along streambeds and banks. This flow is critical to the supply, transport, and storage of oxygen, nutrients, and contaminants in stream ecosystems. "Quantitative assessment of surface-subsurface hydrologic interactions is an essential step in understanding and interpreting the exchange of oxygen, nutrients, and all other constituents between surface water and subsurface zones" (Packman and Bencala, 2000). The "Land-Water Interface" (Figure 1) illustrates the relationship of the hyporheic zone to the ecosystem of the stream and adjacent surface and subsurface.

As with other environmental margins such as forest-prairie, ocean basin-continental shelf, peritidal, and mountain-piedmont, the characteristics of the bounding systems enhance activity at and near the interface. While isolated ground water is sparsely populated, complex communities exist in the hyporheic zone at significant horizontal and vertical distances from contact with surface water, demonstrating the

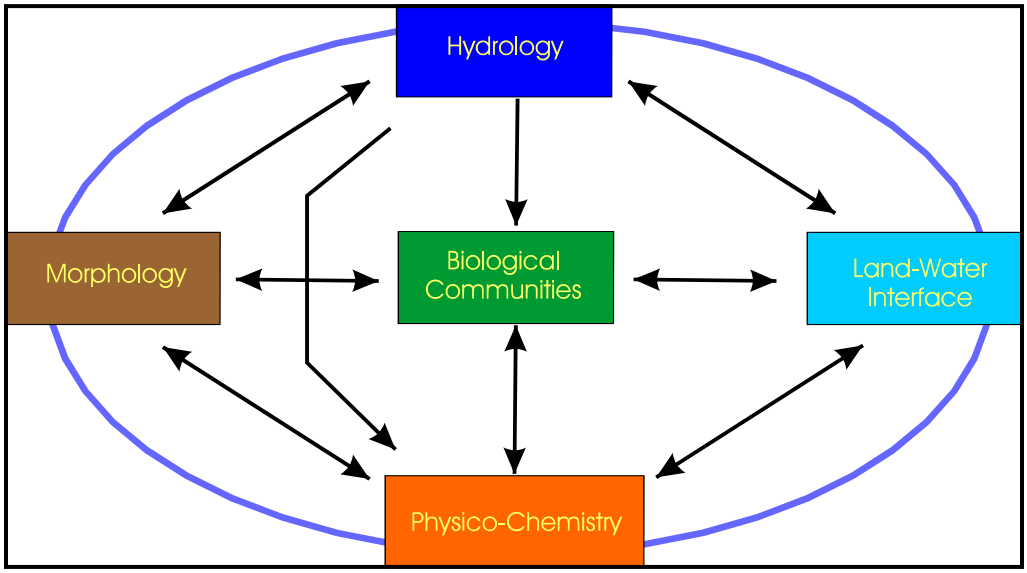

Figure 1: Conceptual schematic of running water ecosystems, modified from Shanahan et al., 2000

extension of a viable habitat beyond the surface water bed (Triska et al., 1989) that can provide a refuge during disturbances such as freeze, flood, or drought (Stanford and Ward, 1993). As the space in which surface and ground water mix, the hyporheic zone is the enhanced environment in which biogeochemical processes profoundly affect the water chemistry (Sophocleous, 2002), influencing stream water concentrations of carbon, nitrogen, oxygen, sulfur, and phosphorous through, for example, organic carbon processing, sulfate and ferric iron reduction, and nitrate reduction (Duff et al., 1998). These processes may control biological activity within stream channels, and "filter" agricultural pollutants from the ground water as they enter the stream system (Stanford and Ward, 1993) when oxidized solutes from the surface water mix and react with reduced solutes from the ground water (Duff et al., 1998) in an environment that may increase contact time between surface water and the underlying geological materials

(Sophocleous, 2002). At a greater range, hyporheic exchange may enhance the nutritional value to riparian plants, which, in turn, mediate such chemical transformations as nitrogen fixation (Stanford and Ward, 1993). Thus, the hyporheic zone plays an essential part in the stream and riparian ecosystems.

To understand the chemistry and biology of the hyporheic zone, it is critical to understand the mechanics of hyporheic exchange and pay close attention to dynamics of the seepage-face boundary conditions (Sophocleous, 2002, Worman et al., 2002). "At a minimum, we need to describe the magnitude and direction of subsurface flows" (Palmer, 1993). Attempts to quantify the flux of water in the hyporheic zone are plagued by heterogeneity and scale problems (Sophocleous, 2002), and traditional methods of measuring surface water-ground water exchange do not work. Seepage-run data, for example, measures reach-averaged net gain or loss by the stream but provides no information on water that enters the stream bed and returns to the stream. Therefore, we must use either tracer tests, or apply Darcy's law to estimate the flux by the distribution of hydraulic head and the highly uncertain estimates of hydraulic conductivity (Harvey et al., 1996). Previous investigations have explored the effects of longitudinal variations in the distribution of head created by bedforms, but nothing has been published describing the effects of lateral variations in flow velocity.

Ground Water Flow and Darcy's Law

Groundwater flow is described by the principles laid out in 1856 by Henry Darcy. In developing a water treatment system for the city of Dijon, France, Darcy

carried out a series of experiments in which he measured the flow of water through columns of sand under varying conditions. The results are expressed in the empirical *Darcy's Law* (Equation 1) that is now used universally in describing water flow through

$$Q = -KA\frac{dh}{dl} \qquad 1$$

$$Q = -\mu\rho g d_{10}\frac{dh}{dl} \qquad 2$$

porous saturated material. The law has been found broadly applicable and the more general form (Equation 2) is now applied to all liquid-phase fluid flow through porous media. In Equation 1, Q is volumetric flux, having units of volume (L^3) over time (T); A is a cross-sectional area (L^2) across which water flows; dh/dl is the hydraulic gradient (L/L), or the difference in the hydraulic head (h) divided by the distance (l) over which the difference in h is measured. The remaining term (K) is the "hydraulic conductivity" of the medium (L/T), and describes the celerity with which it allows the water to flow. It is analogous to "specific conductance," which, as the inverse of resistance, describes the ease with which electricity flows through a material. In that K describes the flow of water, it is a function of water as well as the medium. To describe the flow of other fluids, K is generalized in Equation 2 with the terms μ, fluid viscosity; ρ, fluid density; g, gravitational acceleration; and k, "intrinsic permeability," a constant of proportionality that describes the material alone (Freeze and Cherry, 1979).

Stated simply, a difference in hydraulic head drives flow and a porous medium resists it. The former is expressed in terms of h as a height of a water column; the latter

is expressed as its inverse of its resistance, K in units of length/time. This thesis explores both parameters as they affect the hyporheic zone in a small stream.

Hydraulic head (*h)* is fundamentally the sum of all the energy of the water. The total mechanical energy of a fluid is described by *Bernoulli's Equation* (Equation 3), in

$$P + \rho g h + \frac{1}{2}\rho v^2 = C \qquad 3$$

which P is the static pressure (ML/T^2); ρ is the density (M/L^3); v is the velocity (L/T); g is gravitational acceleration (L/T^2); and z is the elevation (L)of the fluid. In groundwater flow, the v term is negligible and is generally ignored. Other non-mechanical forms of energy—heat, chemical, and electrical, for example—are also generally negligible and not considered. In a flowing stream, however, the v term becomes significant and may be sufficiently large to control the magnitude or even the direction of flow. Chapter 2 tests the hypothesis that the kinetic energy of stream water creates a measurable difference in h.

Hydraulic conductivity, K, is the inverse of the resistance of a porous medium to flow. This parameter is a function of the grain size, shape, and sorting of the medial material. The K-value for even the most uniform material naturally varies over space by up to an order of magnitude. Many *in situ* and laboratory techniques have been developed to estimate K for a material. Most of these techniques are designed in the context of evaluating a subsurface aquifer either as a water source or as a conduit for contaminants, both of which are dominated by horizontal flow. Characterizing hyporheic zone water exchange requires estimating vertical K at a saturated surface. Chapter 3 sets

forth the principles for and tests the application of a new *in situ* technique for estimating the stream bed *K*.

Geologic and Geohydrologic Setting

Data for this study were collected from Little Kickapoo Creek adjacent to the Illinois State University Randolph Well Field, about five miles south of Bloomington and two miles east of U.S. Highway 51 in McLean County Illinois. The specific study site is a meander in the stream (Figure 2) with relatively unobstructed flow, where average linear velocity and discharge vary from an extreme minimum 0.01 m/s and 0.003 m^3/s at base flow to at least 0.80 m/s and 3.86 m^3/s just below flood stage.

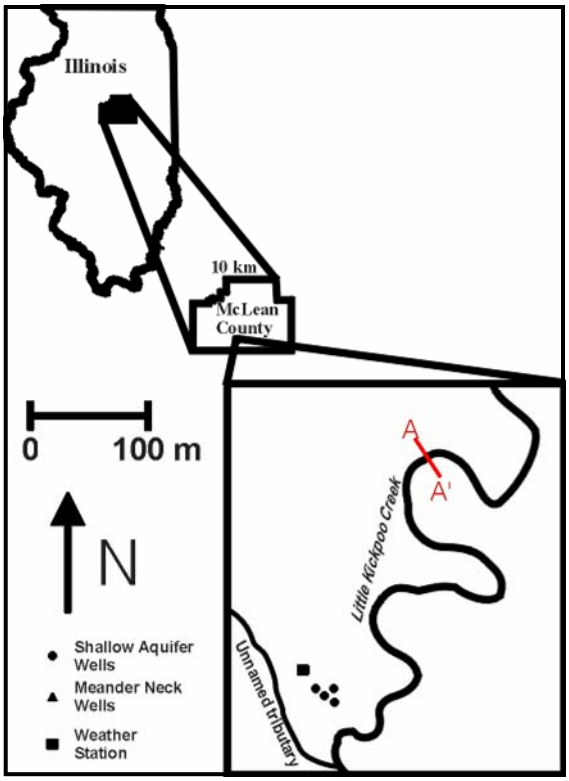

Figure 2: Location of study site.

Little Kickapooo Creek is a low-gradient (0.001, or 10 ft per 1.7 mile, about 6 ft per mile, USGS Bloomington East Quadrangle, 7 ½' Series) third-order perennial stream. It heads about 11 km north of the study site in Bloomington, Illinois, where its own and tributary channels have been modified. The drainage area upstream from the study site is about 52 km^2 (Illinois State Water Survey, 1995). Locally, it is unmodified and meanders through an alluvial valley about 300 m wide. The channel banks range from cut banks sharply incised through the alluvium, to slumps and depositional point bars. The stream bed generally runs just below the top of the Henry Formation (discussed below). Shallow rapid flow channel beds ("riffles") generally consist of gravel and coarse sand with minor interstitial silt. Point bars range from gravel to sand to mud. Relict channels downstream of point bar apices have up to 0.25 m of soft, uncompacted mud. Local pools within hundreds of meters up- or downstream from the study site range up to 1 m below the top of the Henry Formation. Ground water discharge supports perennial base flow in Little Kickapoo Creek on the order of 0.06 m^3/sec, with peak base flow channel velocities up to 0.35 m/sec. The temperate continental humid climate of the Midwest provides frequent showers and occasional heavy rain, especially during the spring and summer. Heavy precipitation events, urbanization in the headwater area, channelized reaches upstream, and ubiquitous agricultural field drain tiles all contribute to rapid, high-magnitude stream response.

A relatively small precipitation event (9/27/2003) generated a peak response within three hours and returned to baseflow within eighteen hours.

LK2C 2003/11/18 04:15 8.622

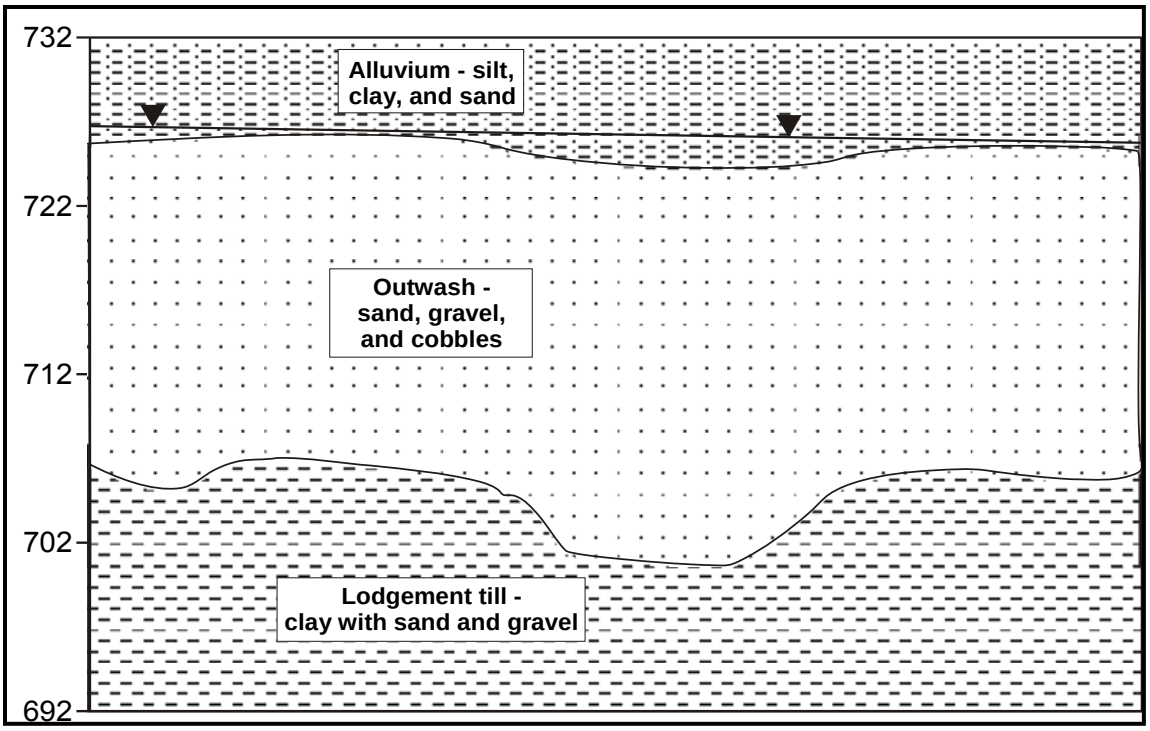

Figure 3: General stratigraphy of the study site.

LK2C 2003/11/18 15:45 9.931

LK2C 2003/11/22 14:45 8.725

A larger precipitation event (11/22/2003: 04:15) generated a 1.3 m increase in stage over 11.5 hours and returned to within 0.1 m of baseflow over the subsequent ninety-six hours (Figure 2.7).

Following a precipitation event that started on 2003 August 31, *LK2C* responded with a 1.1 m rise in stage in twenty hours, then returned to a baseflow pattern and stage over the following forty-eight hours (Figure 2.7).

The study area is within an alluvial valley with numerous end-moraines in a Wisconsonian glacial plain. At the surface are up to 2.1 m of Holocene Cahokia

Alluvium sitting on 5 to 7 m of glacial outwash of the Henry Formation. These surface sediments sit on top of the low-permeability clay-rich lodgement till of the Wedron Formation (Figure 3) which extends to bedrock at a depth of ***XXXXXXX*** m. The area around the study site is used primarily to grow corn and soybeans. The Bloomington Water Reclamation District owns the property, and is constructing a wastewater treatment plant and a wetland about 0.5 km downstream from the study site. The Hydrogeology program at Illinois State University operates and maintains an educational well field on the reclamation district property, about 300 m southwest of the study site. The well field comprises a pumping well screened through the Henry Formation, 3 sets of nested piezometers, each with screens at the water table, at the middle, and at the base of the Henry Formation. An additional 4 piezometers screened through the Henry Formation. Since the wells and piezometers were installed in the summer of 2001, students and instructors from ISU have performed several pump tests and slug tests to determine aquifer properties. The water table in the study area is unconfined and generally varies from 2 to 2.75 m below the land surface, close to the contact between the Cahokia Alluvium and the Henry Formation, and closely follows the Little Kickapoo Creek stream stage. Results of pump tests at the well field indicate that the hydraulic conductivity of the Henry Formation is about 1×10^{-3} m/s (Stephen J. Van der Hoven, personal communication, April 2003).

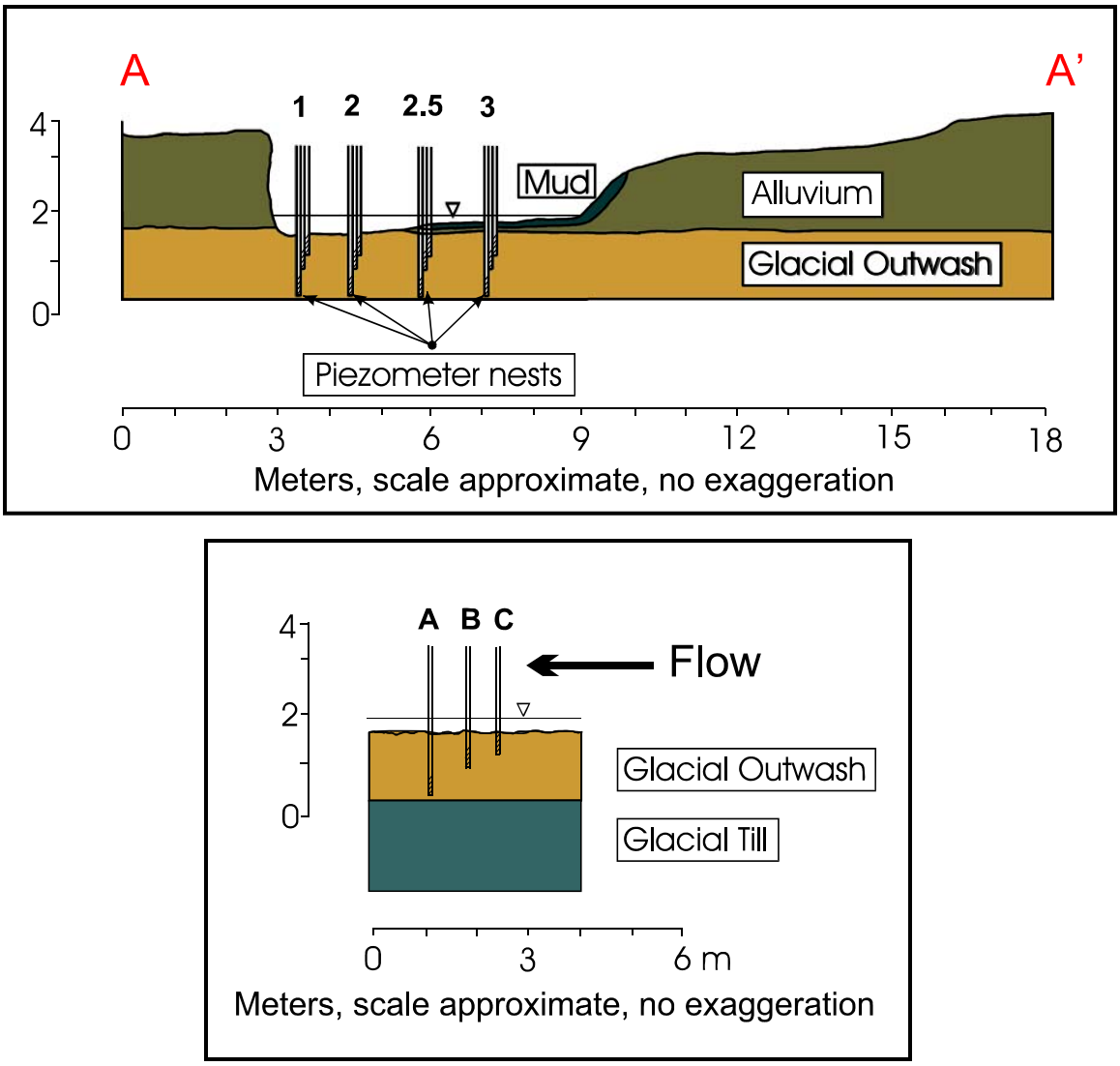

Figure 4 A and B: Schematic diagrams of study site cross-section looking upstream (A) and from the point bar toward the cut bank (B). Transect A-A' is shown in Figure 2.

Manual and Logged Pressure (*h*) Data

Data was collected from three nests of piezometers, ***LK1***, ***LK2*** and ***LK3***, installed in the stream channel. The nests are about 1.5 m apart, arranged perpendicular to flow from the cut bank to the point bar, respectively (Figure 4A and B). Each nest

includes three piezometers arranged parallel to flow direction: ***A***, 1.6 m below the stream bed; ***B***, 0.6 m below the stream bed; and ***C***, 0.1 m below the stream bed. The piezometer screens are commercial 3.2 cm inside diameter steel drivepoints, with 3.2 cm galvanized steel pipe risers. The drivepoints' screen open intervals are restricted with duct tape to 5 cm at the bottom of the ***A***- and ***B***-series drivepoints, and at the top of the ***C***-series drivepoints. Data was collected at 15-minute (900-second) intervals from Druck pressure transducers rated at 0.05 m of water resolution, connected to Telog 2109 data loggers. Stream stage and water table elevation in the piezometers were manually measured periodically with an electrical water-level tape to a resolution of 0.015 m. Because the narrow piezometer pipes prevented consistent placement of the pressure transducers, logged data was calibrated to manual readings.

CHAPTER II

THE EFFECT OF LATERAL DIFFERENCES IN FLOW VELOCITY ON HYPORHEIC INTERCHANGE

Hypothesis

As a stream flows around a meander point, the water flows quickly in the thalweg and near the cut bank, while it flows very slowly along the point bar. This study tests the hypothesis that the difference in flow velocity is great enough to create a measurable *Venturi Effect*, which describes effects of the difference in pressure created by the difference in velocity of the flow of fluids. Bernoulli described the conservation of energy of a streamline with Equation 4:

$$P_1 + \rho g h_1 + \frac{1}{2}\rho v_1^2 = P_2 + \rho g h_2 + \frac{1}{2}\rho v_2^2 \qquad 4$$

where P_1 and P_2 are the pressure of the standing water and the flowing water, respectively, v_1 and v_2 are the velocities, ρ is the density of the fluid, g is gravitational acceleration, and h_1 and h_2 are the elevations of the streamlines (Cutnell et al., 2001.). Venturi described the implication of Bernoulli's equation that, for a given horizontal streamline of a flowing incompressible fluid, the ρgh term does not change. To con-

serve energy as the velocity of the fluid increases, the pressure, *P*, must decrease. At two points of equal elevation in the cross-section of a stream, Equation 4 becomes:

$$P_1 + \frac{1}{2}\rho v_1^2 = P_2 + \frac{1}{2}\rho v_2^2 \quad 5$$

If point 1 is on the point bar side of the stream where the velocity is negligible and point 2 is on the cut bank side of the stream where the velocity is significant, the v_1 term becomes negligible and the equation reduces to:

$$P_2 = P_1 - \frac{1}{2}\rho v_2^2 \quad 6$$

According to this equation, the pressure P_2 on the cut bank side of the stream will be less than P_1 on the point bar side of the stream when there is a significant difference in velocity. Figure 5 shows the theoretical difference in head between standing and flowing water as a function of water velocity for steady laminar flow. This study tests the hypothesis by measuring the pressure in the shallow subsurface below the stream bed, measuring the stream water velocities at the piezometers, and examining the data for a correlation between stream water velocity and differences in head between the piezometers.

The null hypothesis is that the velocity of flow in the stream does not create a measurable Venturi Effect. If the velocity term is negligible, Equation 4 becomes:

$$P_2 = P_1 \quad 7$$

for stream lines at the same elevation .

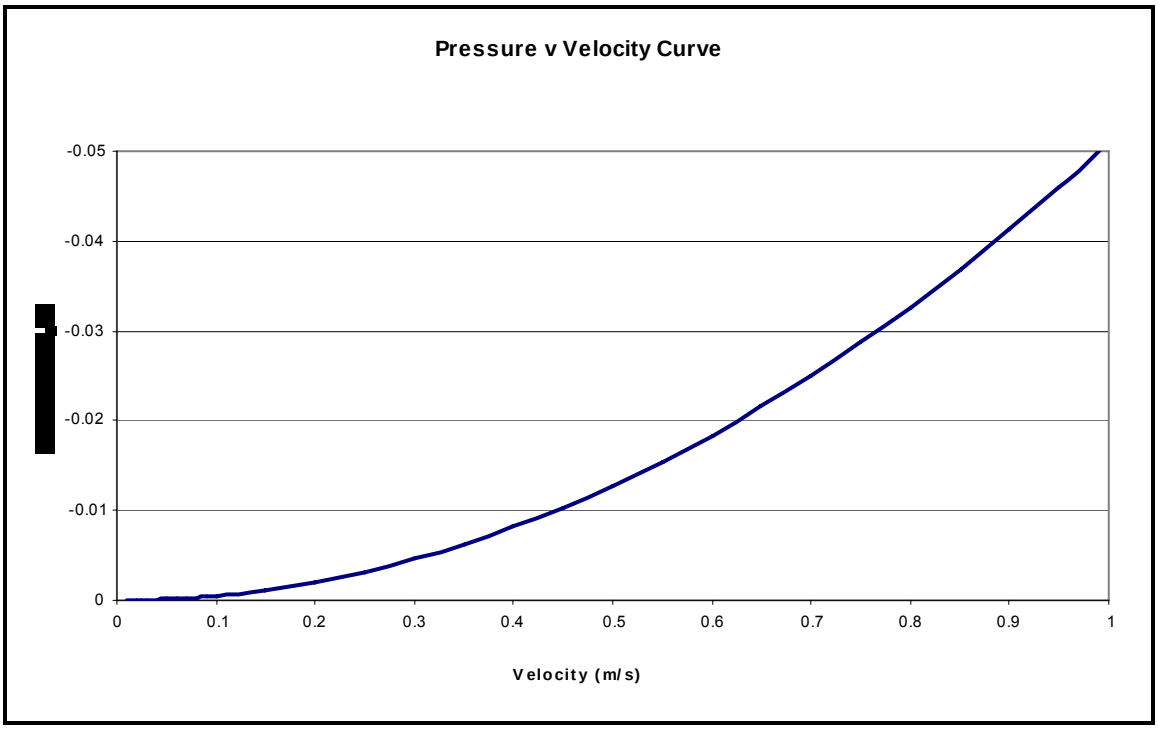

Figure 5: Theoretical difference in head as a function of velocity.

Vertical Stream Velocity Distribution

Stream water velocity varies both laterally and vertically within a cross section perpendicular to flow.

Data

Baseflow stream velocity measurements show that near the cut bank along the line of ***LK1*** velocity is about 0.3 m/s, while in the middle of the stream and near the point bar along the lines of ***LK2***, ***LK2.5*** and ***LK3*** the velocity is near zero or is negative (Figure 6). As the stream stage increases, velocity increases by a factor of less than two from about 0.4 to about 0.7 m/s for ***LK1***; along the lines of the remaining piezometers, ***LK2***. The multiplier for the increase in velocity for ***LK3*** cannot be calculated, but in-

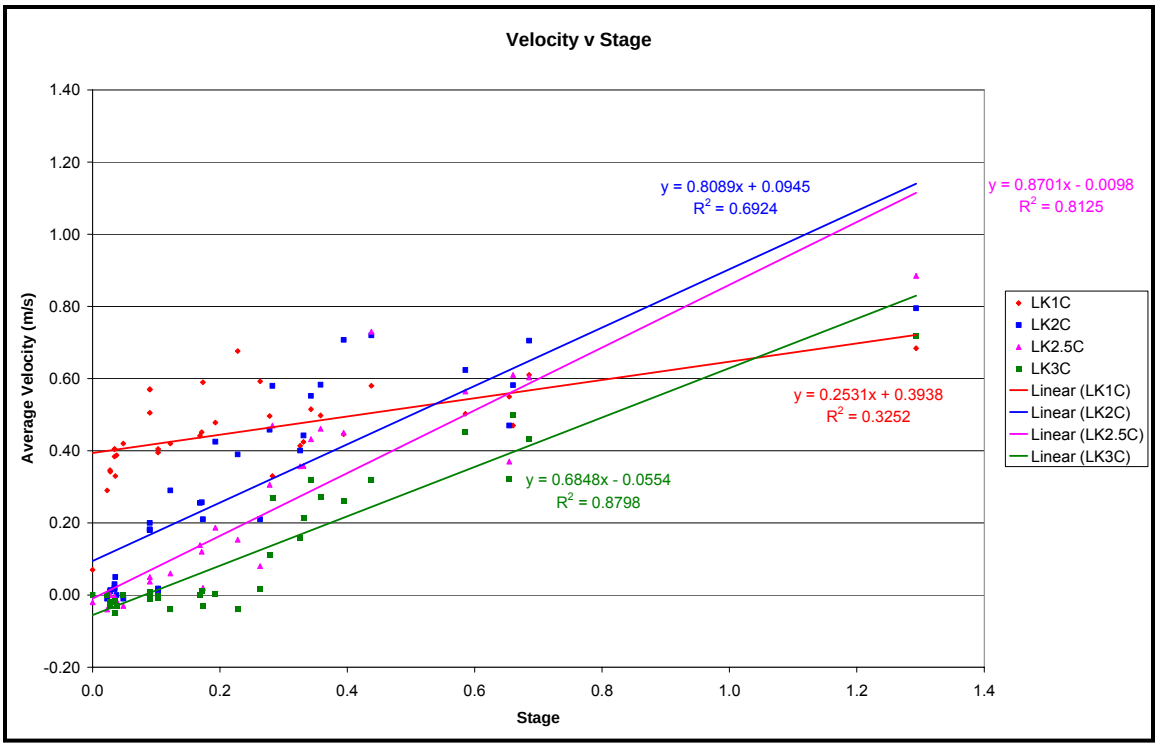

Figure 6: Stream velocity at piezometer nests as a function of stage, with zero-elevation set at lowest measured stage.

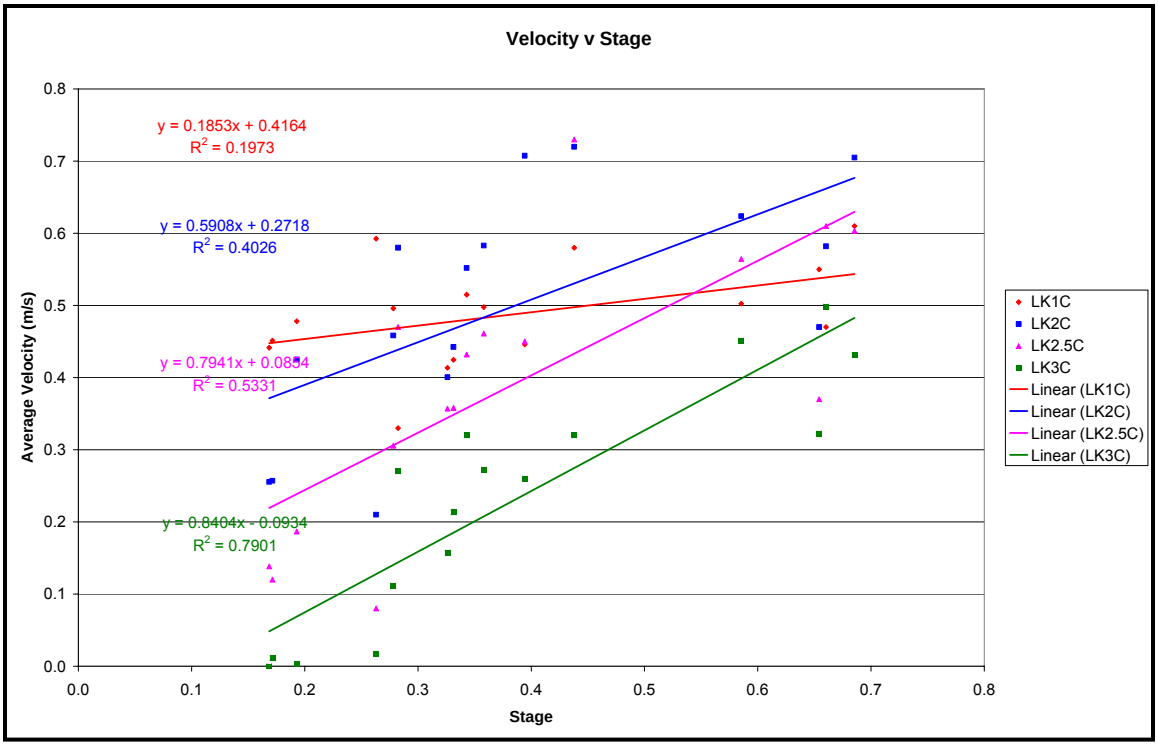

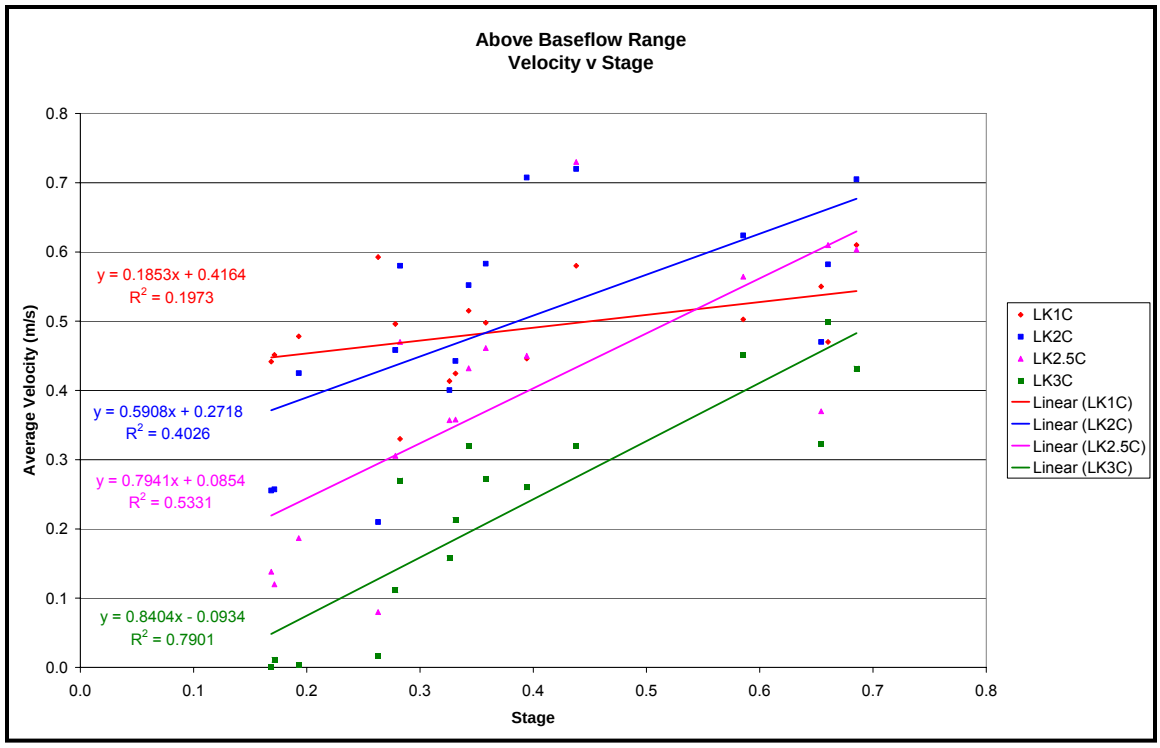
Above Baseflow Range
Velocity v Stage
y = 0.1853x + 0.4164
R2 = 0.1973
y = 0.5908x + 0.2718
R2 = 0.4026
y = 0.7941x + 0.0854
R2 = 0.5331
y = 0.8404x - 0.0934
R2 = 0.7901
Average Velocity (m/s)
Stage
LK1C
LK2C
LK2.5C
LK3C
Linear (LK1C)
Linear (LK2C)
Linear (LK2.5C)
Linear (LK3C)

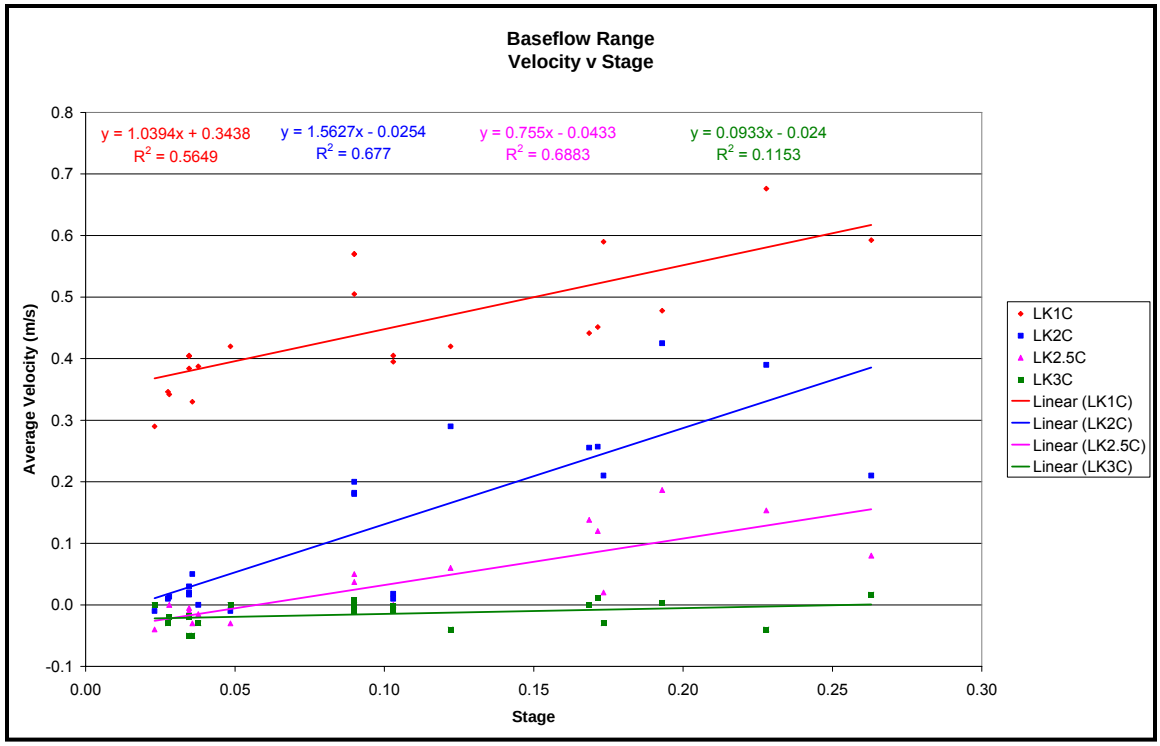
Baseflow Range
Velocity v Stage
y = 1.0394x + 0.3438
R2 = 0.5649
y = 1.5627x - 0.0254
R2 = 0.677
y = 0.755x - 0.0433
R2 = 0.6883
y = 0.0933x - 0.024
R2 = 0.1153
Average Velocity (m/s)
Stage
LK1C
LK2C
LK2.5C
LK3C
Linear (LK1C)
Linear (LK2C)
Linear (LK2.5C)
Linear (LK3C)

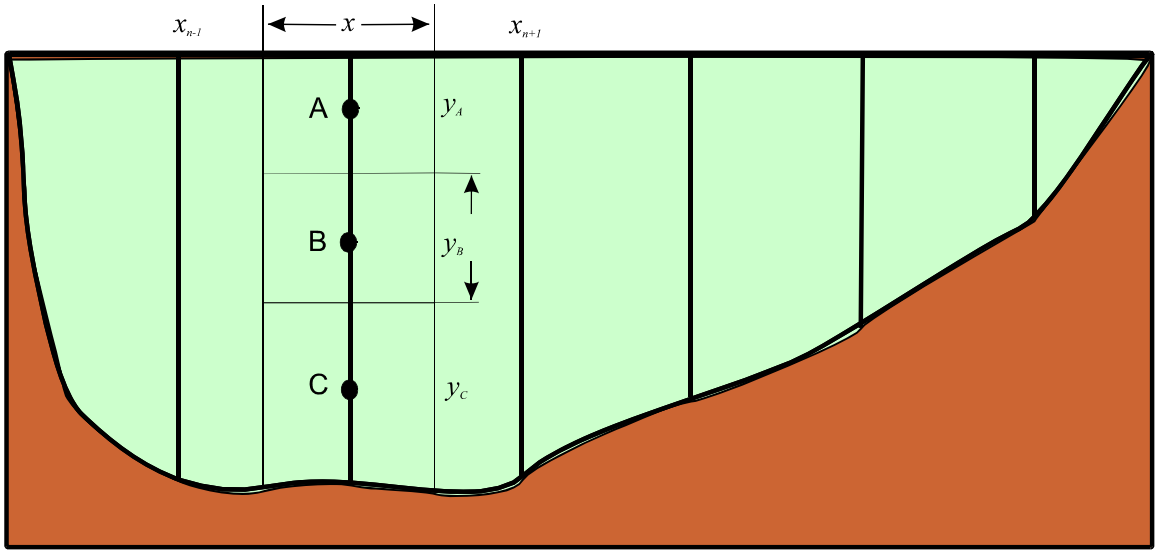

Figure 7: Schematic of stream profile, velocity measurement points, and discharge calculation variables.

Table 1: Duplicate and triplicate calculated discharge with mean, standard deviation, and coefficient of variation showing repeatability of technique. Data sets for analysis were selected based on completeness.

	13-Sep	**14-Sep**	**18-Sep**	**26-Oct**	**24-Nov**	**29-Nov**
a	0.0723	0.1958	0.0610	0.1006		0.2678
b	0.0749	0.1916	0.0660	0.1061	0.7727	0.2536
c		0.1825	0.0609		0.7564	
d	0.0730				0.7353	
average	0.0734	0.1900	0.0627	0.1033	0.7548	0.2607
stdev	0.0013	0.0068	0.0029	0.0039	0.0188	0.0101
CV	0.018	0.036	0.046	0.038	0.025	0.039

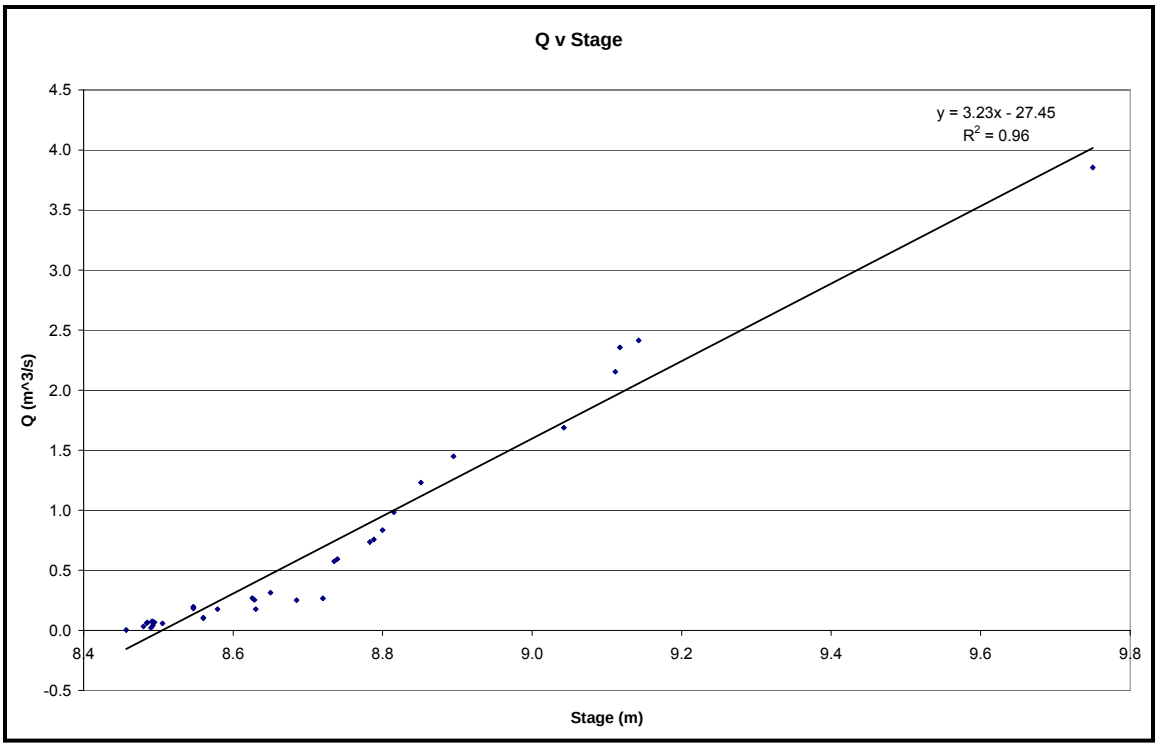

Figure 8: Plot showing linear increase of discharge (Q, m^3/s) versus stage (m, local vertical datum). Coefficient of determination ($r^2 = 0.96$) is for all data points; without the influential point at stage = 9.75 m, $r^2 = 0.94$.

creases from near 0 to 0.7 m/s. Also as stream stage increases, the thalweg (path of highest velocity flow) migrates from the line of ***LK1*** to the line of ***LK2***; at very high flow regimes beyond the measured velocity range, flow appears to be fastest along the line of ***LK2.5***. At base flow and low flow regimes, the point bar creates a low velocity eddy in its lee.

Stream Velocity Profiles

Stream velocity and stage were measured forty-five times, including duplicates and triplicates, over the period from July 9 through November 29, 2003 using a Marsh-McBirney *Flo-Mate 2000*® electromagnetic velocity meter. Velocities were measured

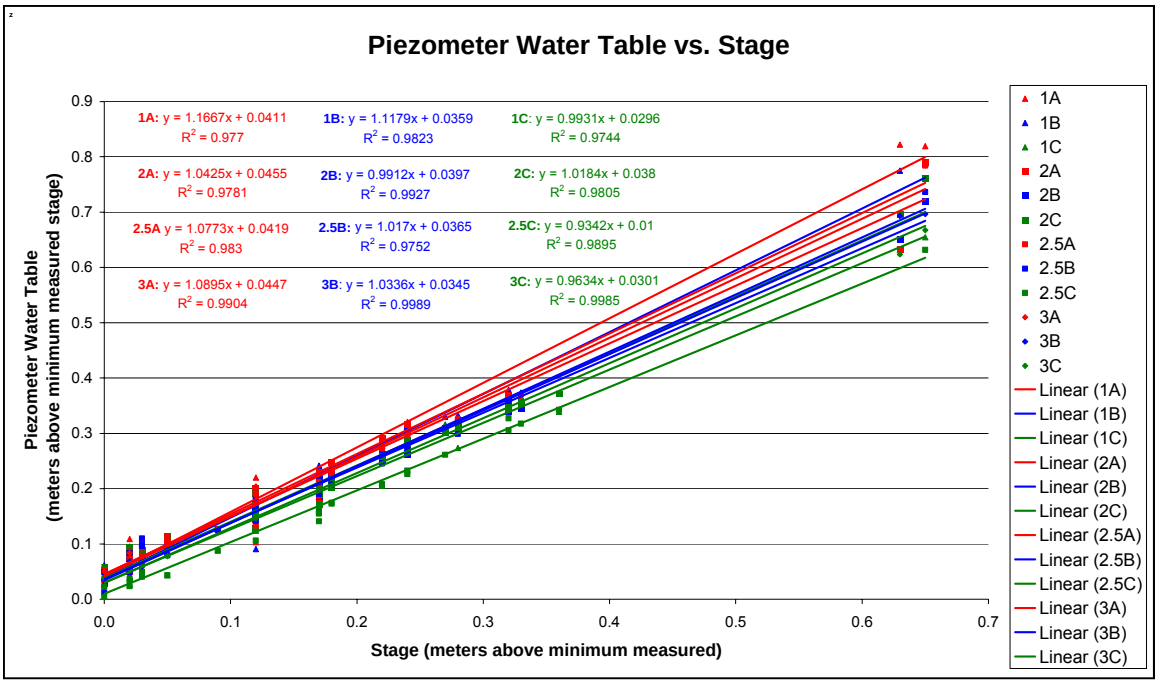

Figure 9***XXXX***: Plot of data points and trendlines showing change of manually measured piezometer water tables versus the stream stage, both as measured above the minimum stream stage. Note that the water tables in the deepest piezometers (***A***-series, in red) are consistently greater than 1; in the intermediate piezometers (***B***-series, in blue) are generally very close to 1; and in the shallow piezometers (***C***-series, in green), are generally less than 1.

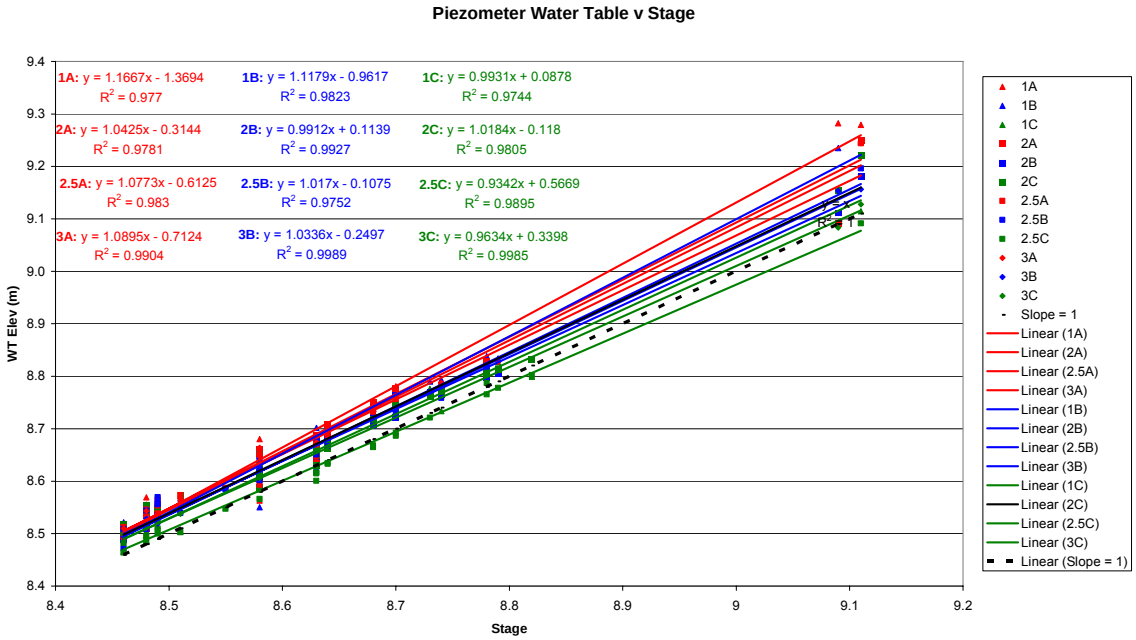

Same data as Figure 2.5, but with trendlines. [From *LKC Velocity Profiles (2005a).xls*, sheet *M v Stage Trends (4)*, 2005 Jun 4.] Notice the grouping of the slopes of the trendlines, i.e., the ***A*** series generally have a higher slope than the ***B*** series which is generally higher than the ***C*** series. The table below shows the data.

Does this mean anything??!? This, along with the charts on the following page, seem to ***suggest*** that

1) as stream stage increases, water tables in the deep wells increase more than the water table in the shallow wells.

2) water tables in the wells on the cut bank side (***LK1*** and ***LK2***) increase more than the water table where the velocity increases the most (***LK2.5***).

Trendline analysis

slopes	A	B	C	average	stdev	CV
1	1.1667	1.1179	0.9931	1.0926	0.0895	0.0819
2	1.0425	0.9912	1.0184	1.0174	0.0257	0.0252
2.5	1.0773	1.0170	0.9342	1.0095	0.0718	0.0712
3	1.0895	1.0336	0.9634	1.0288	0.0632	0.0614
average	1.0940	1.0399	0.9773			
stdev	0.0524	0.0548	0.0365			
CV	0.0479	0.0527	0.0373			

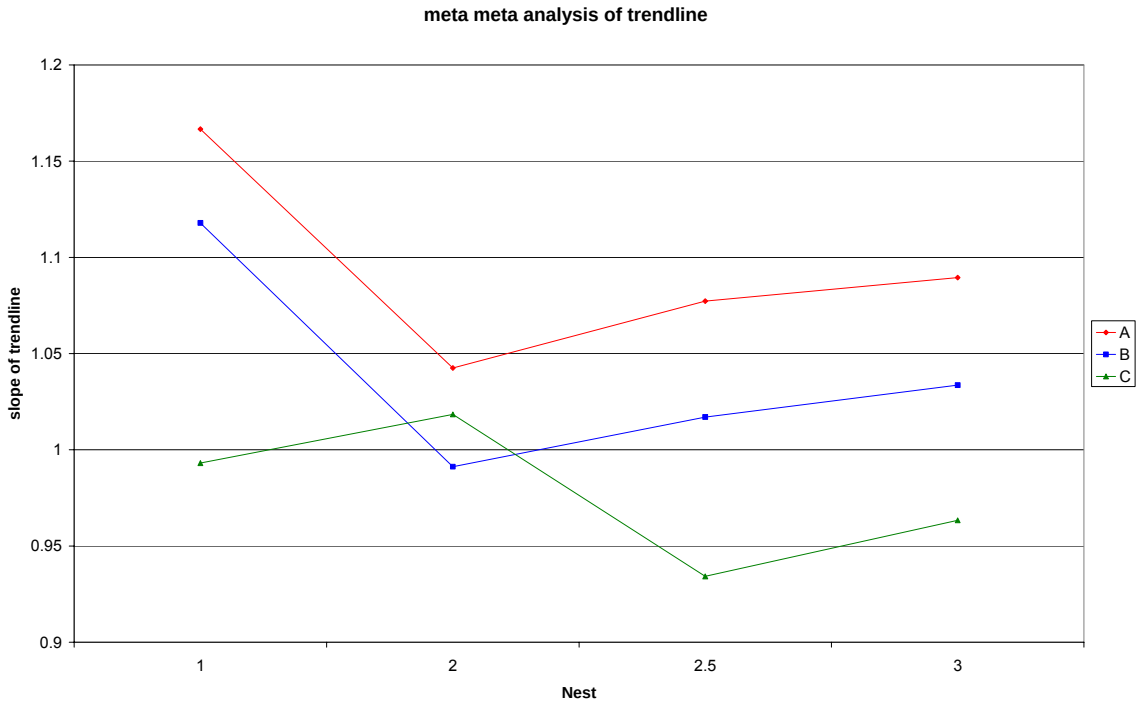

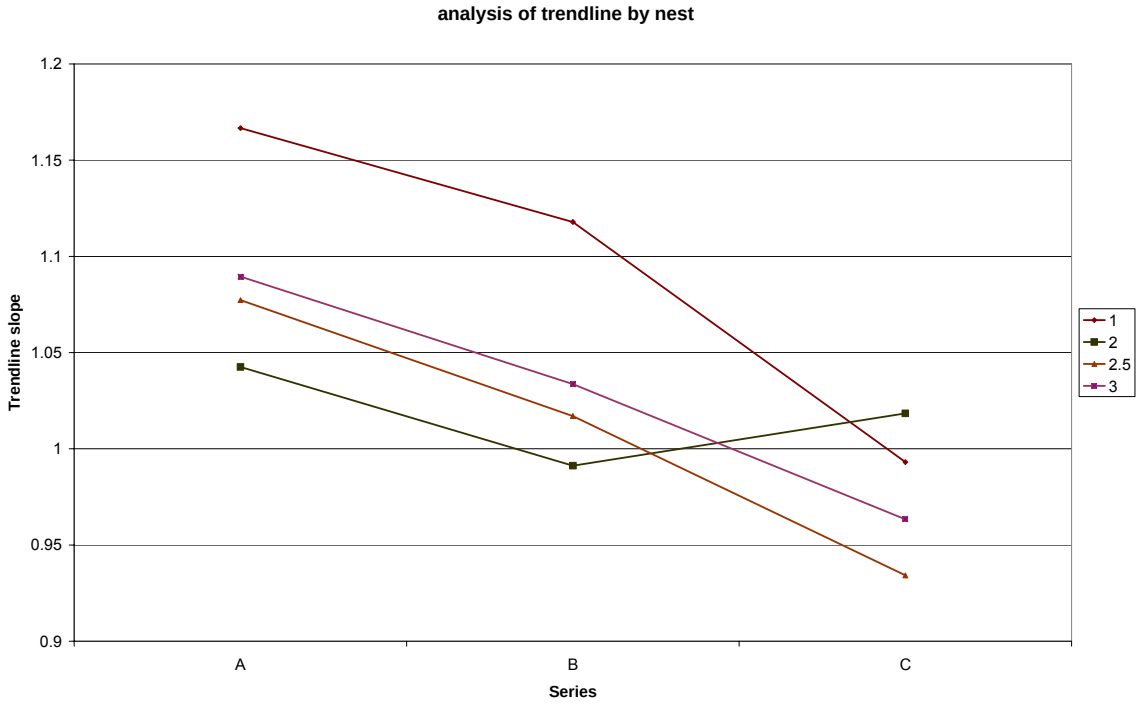

From *LKC Velocity Profiles.xls; Anlz Trendline 1* and *Anlz Trendline 2*. These show the slopes of the trendlines of the manual piezometer water table elevations plotted against the stream stage. They appear to me to imply something! Top: deep wells increase more than shallow wells (red, A, always higher slope). Bottom: Cut bank (1) generally increases more than the others.

at horizontal offsets along the stream transect directly upstream from each piezometer nest and at other arbitrarily-spaced points. The latter points were selected to adequately represent stream velocities and discharge, based on the flow patterns. For example, velocities varied from zero to 0.6 m/s within a meter of the cut bank, but would be nearly constant over a distance of 1.5 m approaching the point bar. Therefore, data density is higher adjacent to the cut bank than the point bar. At each horizontal offset, velocities were measured at multiples of 0.05 or 0.10 m below the stream surface, and at 0.03 m above the bed. Stage was calculated using the distance of the stream surface below the surveyed elevation of the tops of the piezometer pipes. Discharge was calculated as the velocity measured at the center of an element times the cross-sectional area of the element. The element is defined as the area between vertical lines halfway between horizontal offsets and horizontal lines half the distance between measurement depths (Figure 7). The cross-sectional area used to calculate discharge for the element including point B equals x time y_B. The distance x is calculated as half the distance from the previous to half the distance to the next vertical line on the transect. The vertical distance y_B is calculated as starting at half the distance from A to B and ending at half the distance from B to C. The vertical distance for A is calculated as the depth of A plus half the distance to B. Total stream discharge was calculated as the sum of the discharge of the measured elements. Average linear velocity was calculated as the discharge divided by the total cross-sectional area. Discharge ranged from 0.003 m^3/s to 3.9 m^3/s as stage varied by 1.3 m, and average linear velocity varied from 0.01 m/s to 0.80 m/s. Discharge increases linearly with stage (Figure 8) for the measured range

(n=36, r^2 = 0.96). Four triplicate and two duplicate measurements were collected to determine precision (Table 2.1). The coefficient of variation of the measurements ($s/\bar{x}$) ranged from 0.02 to 0.05 over a discharge range of 0.06 to 0.77 m^3/s, showing that the instruments and technique yield highly reproducible results.

Manually Measured Head Data

The stream stage and piezometer water level elevations were manually measured on 31 occasions in the period from July 8, 2003 through April 29, 2004 (Figure 9) *[optional addendum/appendix? And another appendix for velocity data?]*. Of these, two sets of measurements—both collected on July 9, 2003, following a 100-year precipitation event—were discarded due to suspected inaccuracies resulting from the extreme conditions under which they were taken. On the remaining occasions, partial data sets—i.e., head measurements from some but not all piezometers—were collected. *[Sometimes due to time constraints, other times due to technical difficulties, e.g., damaged piezometers.]* All manual measurements were taken from the surveyed tops of the piezometer pipes. On 25 occasions, multiple (two to eight) measurements of the stream stage were collected from different piezometer pipes. Of these, on 19 occasions, the standard deviation of the measurements was less than 0.01 m; on one occasion, the standard deviation was 0.026 m. In the field, the practical accuracy of the manual measurements is ±0.02 m.

Statistical analyses by Pearson's product moment correlation of manually measured piezometer head and stream stage data are presented in Tables 2 through 4. Table 2 shows that water level in the piezometers correlates to stream stage with a mini-

Table 2: Pearson's product moment correlation of piezometer water tables with stage, by nest.

	r	*n*
1A	0.988	18
1B	0.991	25
1C	0.987	26
2.5A	0.991	24
2.5B	0.988	20
2.5C	0.995	27
2A	0.989	18
2B	0.996	25
2C	0.990	26
3A	0.995	15
3B	0.999	10
3C	0.999	10

Table 3: Pearson's product moment correlation of stage with (stage minus manually measured piezometer water table elevation) by nest (A) and by series (B)

3A

	r	*n*
1A	-0.68	18
1B	-0.62	25
1C	0.04	26
2A	-0.26	18
2B	0.10	25
2C	-0.13	26
2.5A	0.75	24
2.5B	-0.10	20
2.5C	0.56	27
3A	-0.64	15
3B	-0.71	10
3C	0.70	10

3B

	r	*n*
1A	-0.68	18
2A	-0.26	18
2.5A	0.75	24
3A	-0.64	15
1B	-0.62	25
2B	0.10	25
2.5B	-0.10	20
3B	-0.71	10
1C	0.04	26
2C	-0.13	26
2.5C	0.56	27
3C	0.70	10

mum *r*-value of 0.987, indicating that within the time period and spatial resolution of measurement, the subsurface water pressure and the stream stage respond synchronously in the same direction, and suggests that the magnitude of the response in the wells scales directly to the magnitude of the change in stream stage and the scaling factor is close to unity. The data analyzed for Table 3 are the differences between stream stage and piezometer water table elevations, presented in nest (A) and series (B) order: the analysis shows no consistent pattern of correlation. *[Table 2.4, 13 of 18 positive correlation. Deep minus shallow, cut bank minus point bar.]* The data analyzed for Table 4 are differences between water table elevations in piezometers. The differences are calculated as "proximal to the cut bank" minus "distal to the cut bank," and "deeper" minus "shallower." Having positive *r*-values for five of six tests among the ***A***-series deep

Table.4 A and B: Pearson's product moment correlation between stream stage and the difference between two wells sorted by series (A) and by piezometer nest (B).

4A

	r	*n*
1A-2A	0.50	18
1A-2.5A	0.22	17
1A-3A	0.68	14
2A-2.5A	0.38	17
2A-3A	0.64	14
2.5A-3A	-0.17	14
1B-2B	0.70	25
1B-2.5B	0.39	17
1B-3B	0.96	10
2B-2.5B	-0.24	17
2B-3B	-0.42	10
2.5B-3B	0.48	9
1C-2C	-0.11	26
1C-2.5C	0.37	24
1C-3C	0.30	10
2C-2.5C	0.46	24
2C-3C	0.83	10
2.5C-3C	-0.41	9

4B

	r	*n*
1A-2A	0.50	18
1B-2B	0.70	25
1C-2C	-0.11	26
1A-2.5A	0.22	17
1B-2.5B	0.39	17
1C-2.5C	0.37	24
1A-3A	0.68	14
1B-3B	0.96	10
1C-3C	0.30	10
2A-2.5A	0.38	17
2B-2.5B	-0.24	17
2C-2.5C	0.46	24
2A-3A	0.64	14
2B-3B	-0.42	10
2C-3C	0.83	10
2.5A-3A	-0.17	14
2.5B-3B	0.48	9
2.5C-3C	-0.41	9

piezometers suggests that as stream stage increases, subsurface pressure increases proximal to the cut bank more than it does distal to the cut bank. Positive values for four of six tests for the ***B***- and ***C***-series piezometers more weakly support the same conclusion.

Table 4B shows that for piezometers of equal depth, the ***LK1*** nest increases with stage by more than the other nests in eight of the nine tests; ***LK2*** piezometers increase greater than ***LK2.5*** and ***LK3*** in four of six tests; and ***LK2.5*** piezometers increase greater than ***LK3*** in only one of three tests. Together, these suggest that 1) changes in head in deep piezometers correlate more closely with stream stage than do changes in head in shallow piezometers, and 2) changes in head in piezometers proximal to the cut bank

correlate more closely with stream stage than do piezometers distal to the cut bank. *[Or do I have all this jumbled up? I am looking at the correlation between* ***X=stream stage*** *and* ***Y=(stream stage minus piezometer water table)****. Or am I looking at* ***X=(stream stage minus water table A)*** *and* ***Y=(stream stage minus water table B)****?]*

Logged Head Data

Nine Telog 2109 data recorders logged data from Druck pressure transducers at 15-minute intervals during the period from July 1993 to April 2004. One set of three instruments was moved from the ***LK3*** nest to ***LK2.5*** in January 2004 to attempt to capture subsurface data along the highest velocity flowpath. Data is occasionally missing due to technical difficulties. The practical resolution of the pressure transducers is 0.03 m (1.2 inches). Table 5 summarizes the logged data.

Table 5. Summary statistics of logged piezometer data.

Piezometer	Begin	End	Count	μ	σ
LK1A	2003-07-09	2004-04-08	25572	8.70	0.22
LK1B	2003-07-09	2004-04-08	26529	8.67	0.21
LK1C	2003-08-28	2004-04-08	21424	8.68	0.17
LK2A	2003-07-09	2004-04-08	21746	8.63	0.24
LK2B	2003-07-09	2004-04-08	26527	8.63	0.22
LK2C	2003-07-09	2004-04-08	26235	8.66	0.22
LK2.5A	2004-01-02	2004-04-08	9280	8.60	0.15
LK2.5B	2004-01-02	2004-04-08	9215	8.64	0.16
LK2.5C	2004-01-02	2004-04-08	9283	8.97	0.24
LK3A	2003-07-09	2004-01-02	16138	8.67	0.26
LK3B	2003-07-09	2004-01-02	16977	8.69	0.26
LK3C	2003-07-09	2004-01-02	16982	8.64	0.32

The narrow diameter of the piezometer pipes and the stiffness of the data cables also made it difficult to accurately and reliably place and replace the pressure transducers in the piezometers. This, along with the coarse resolution of the instruments make direct statistical analysis of the entire dataset meaningless. However, graphs of selected periods where data are self-consistent provide opportunities for some qualitative interpretation.

Graphs of logged piezometer head data are presented by piezometer nest (***LK1*** through ***LK3***) in Figures 10 through 12, and by depth series (***A*** through ***C***) in Figures 13 through 22. Figures 10 through 15 show three months of data, first comparing the different depths within a single nest, then comparing data collected from piezometers at the same elevation laterally across the stream. Difficulties with the calibration of the pressure transducer and logger cause exaggerated responses for the data from ***LK3C*** in figures 12 and 15. To mitigate the extremes, figure 16 shows a running average of the 24 previous, the current, and the 24 subsequent readings (total 49 data points over a period of about 12 hours), contrasted with raw data in figure 17. All piezometers show nearly identical response and peak pressures for the high-stage period on September 1, but that during and following the recession, head in ***LK3C*** falls below and remains consistently lower than the pressures in ***LK1C*** and ***LK2C***. These plots also clearly show the diurnal variation. *[Note: if the calibration, but not the scaling, is off—that is, if pressure in LK3C was actually above the other two wells, with water calm at LK3C and flowing at 1C & 2C—then this would support the hypothesis that flow reduces net downward pressure. At the peaks of the diurnal cycle, water would be the highest and flowing the fast-*

est and affect 1C & 2C; water would be high and not *flowing over 3C, creating higher net pressure.]* Figures 18 and 19 show ***B***- and ***C***-series data for the flood event of July 1993. Hazardous conditions prevented direct observations. The logged data suggest that the pressure in ***LK1B*** was lower than the pressure in ***LK1C***, contrary to the general trend established by manual measurements. Figures 21 through 23 show data for the ***A***-, ***B***-, and ***C***-series wells for July and August 1993. The data have been normalized to manually measured piezometer water table elevations. Aberrant artifacts of unknown origin persist in the data, as demonstrated by ***LK1B*** from September 2 through September 4, 2003 in Figures 10 and 14, and the offset of ***LK3C*** on August 3, 2003 in Figure 16. Also, irregularities were noted when calibrating the instrument initially installed in ***LK3C,*** which was later moved to ***LK2.5C***. These irregularities manifest themselves as an unpredictable sensitivity to head changes in some ranges, and show up on the graphs as exaggerated fluctuations. Debris in the stream frequently caught on the piezometer pipes, scouring the streambed along the study transect; and occasionally snagged the data cables, displacing (lifting) the pressure transducers in the piezometers which manifest as abrupt offsets in the data.

The long-term time series plots do not show any consistent trends or patterns of higher or lower head by nest (***LK1***, ***LK2***, ***LK2.5***, or ***LK3***) or by series (depth, ***A***, ***B***, or ***C***) for the peaks or troughs.

Discussion

Manually measured head measurements and the logged piezometer head data show no trend or pattern of different magnitudes of changes as stream stage increases within the precision of the measurements . Visual inspection of the logged data graphs show that head varies uniformly with stage across the stream. Statistical analysis of manual measurements shows nearly perfect correlation of piezometer water table elevations with stage, and no pattern of correlation of differences between piezometer water table elevations.

Conclusions

As Figure 2.1 shows, the theoretical maximum deviation of measurable vertical pressure for the greatest.

The maximum measured difference in velocity was observed on September 4, 2003, when the difference in velocity between ***LK1*** and ***LK3*** was about 0.7 m/s. At this difference in velocity, the theoretical difference in head would be on the order of 0.025 m, according to equation 6. This difference is too small to observe with the resolution of the logging instruments used in this study, and at the limit of the resolution of the manual measurements. Therefore, the data, as collected, are inadequate to address the question presented in the hypothesis.

In retrospect, it would have been desirable but probably not practical to better characterize the study site before selecting and installing instruments. Investigators had unrealistic expectations of the maximum stream velocity and stream velocity distribution. This information could be gained prior to the study only by delaying the study.

Therefore, the results of this study are useful insofar as they constrain the upper limit of the potential effect of stream velocity on the direction and magnitude of hyporheic inter-change, and give guidance to future studies at the same or similar sites.

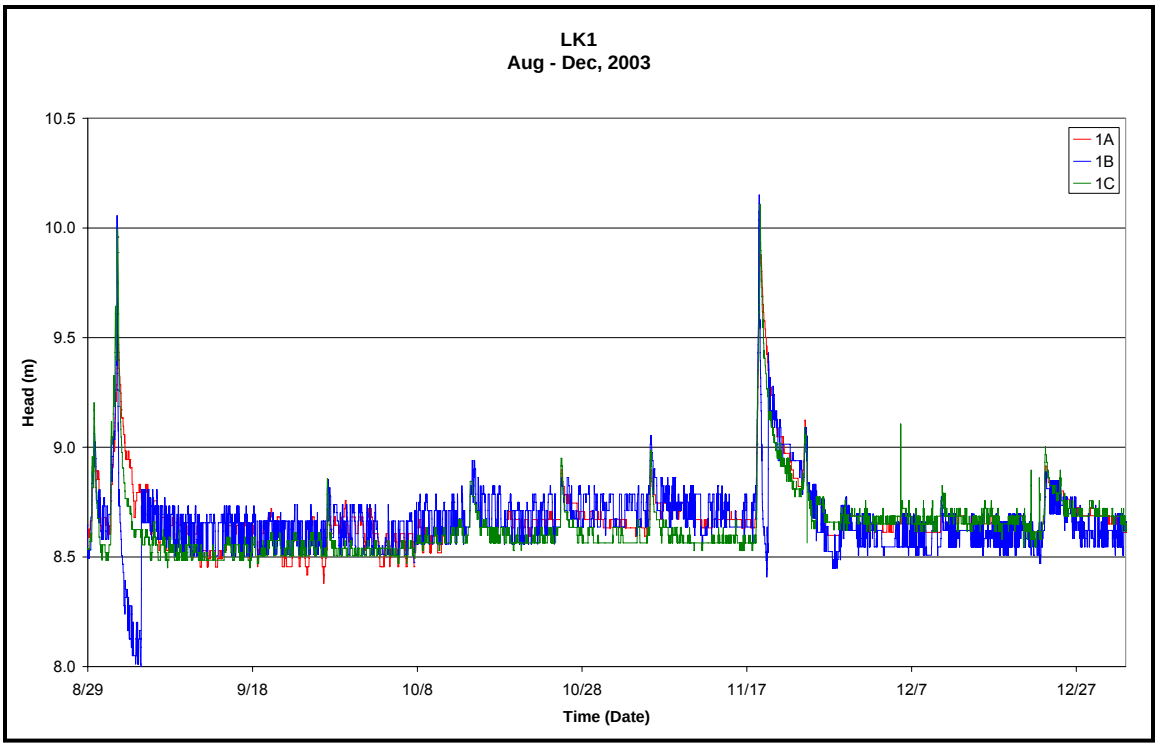

Figure 10: Piezometer Nest LK1 logged head measurements, August-December, 2003.

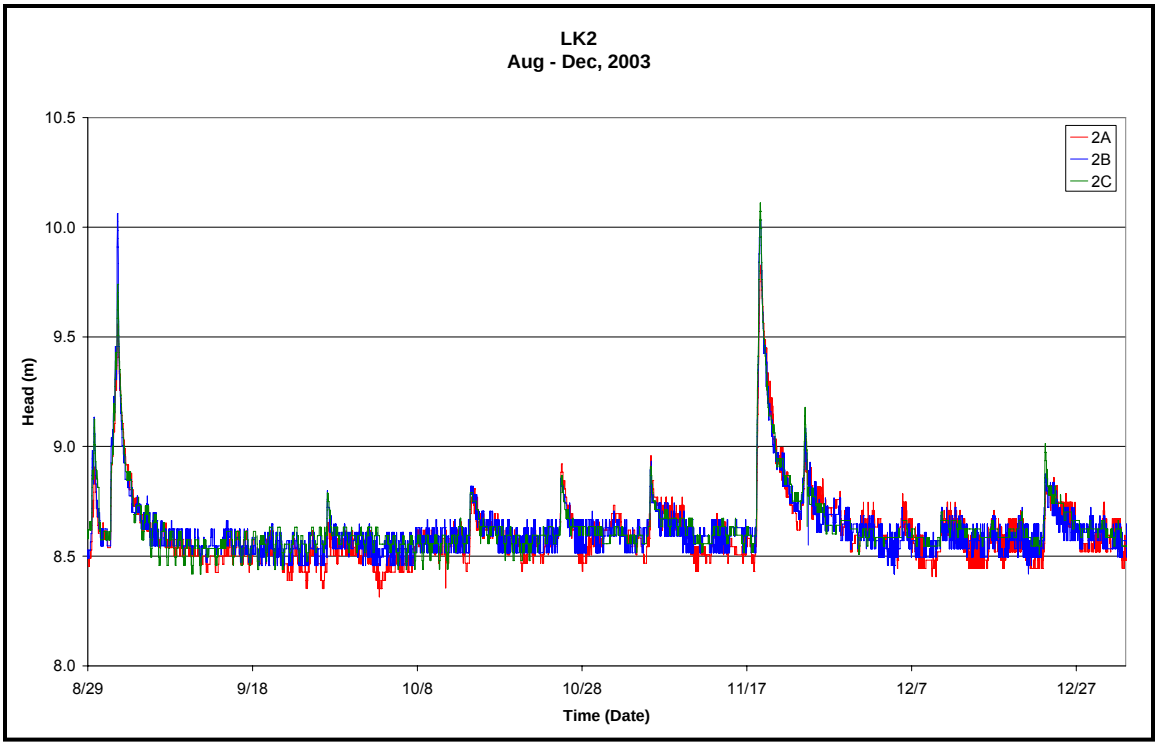

Figure 11: Piezometer Nest LK2 logged head measurements, August-December, 2003.

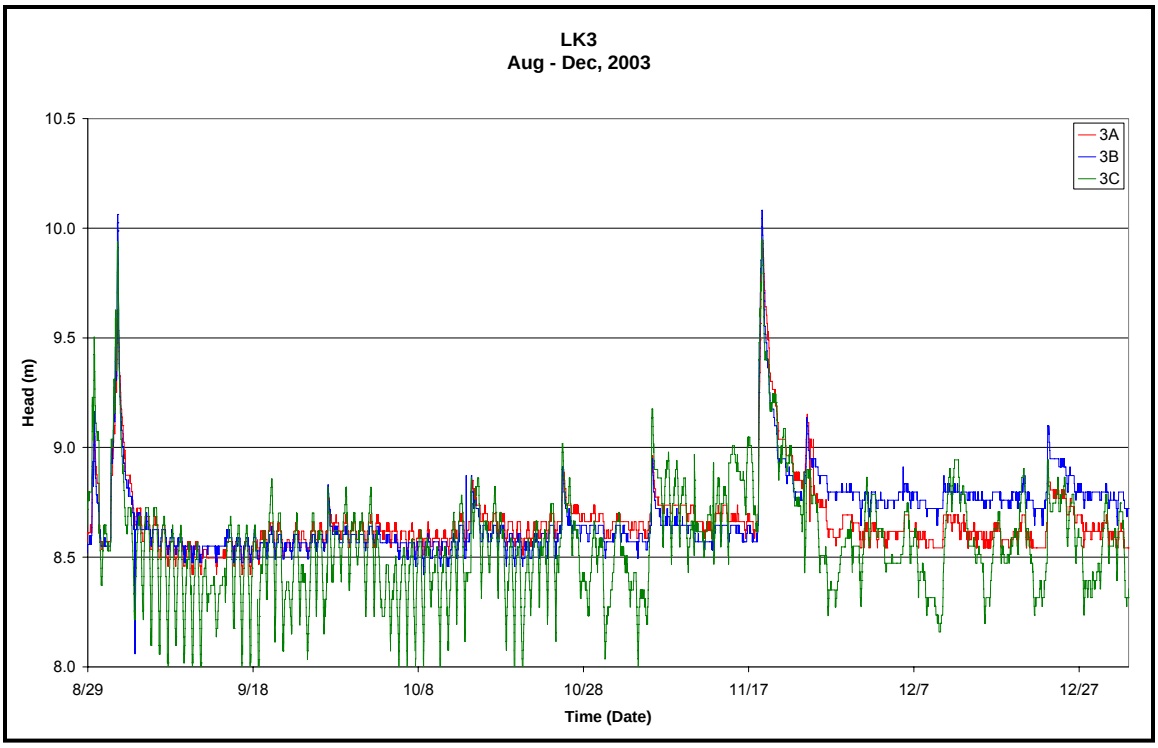

Figure 12: Piezometer Nest LK3 logged head measurements, August-December, 2003.

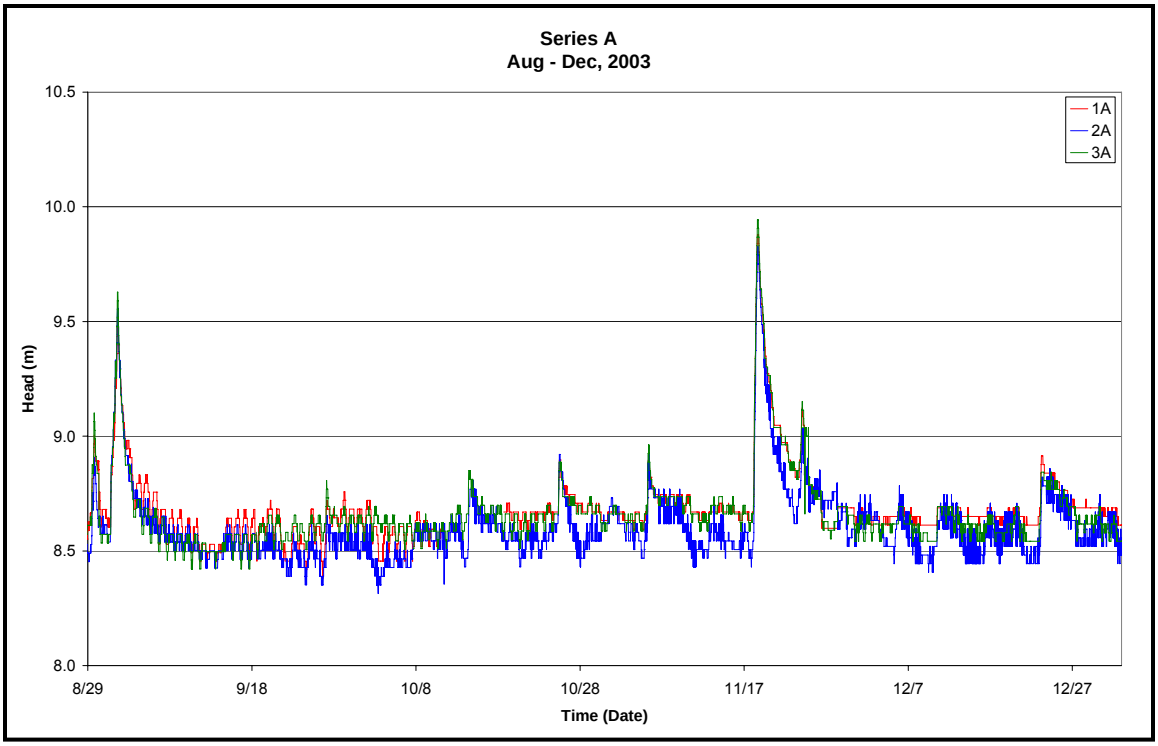

Figure 13: Series A piezometers logged head measurements, August-December, 2003.

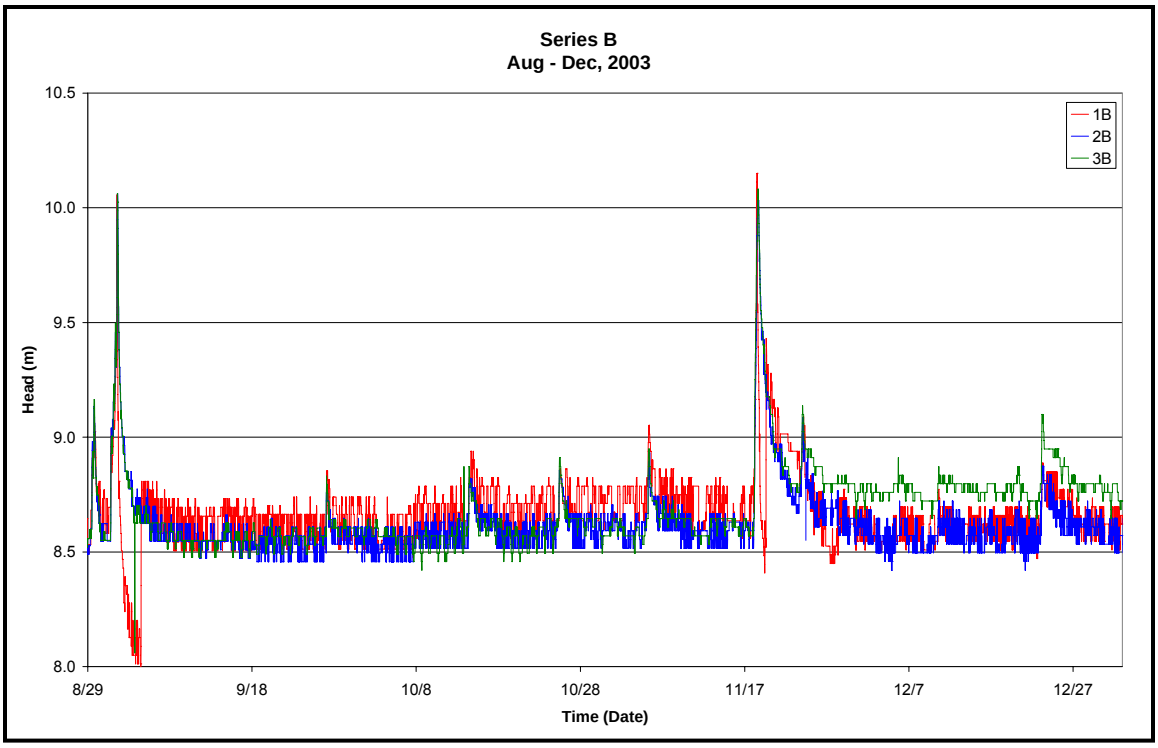

Figure 14: Series B piezometers logged head measurements, August-December, 2003.

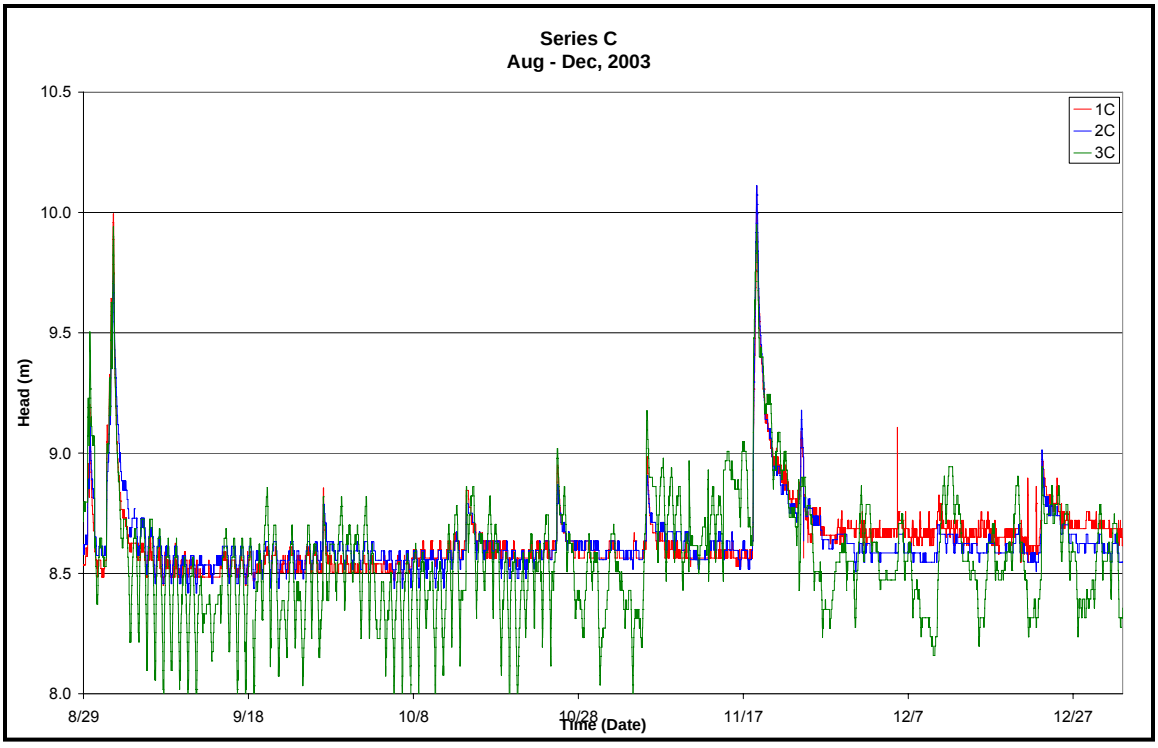

Figure 15: Series C piezometers logged head measurements, August-December, 2003.

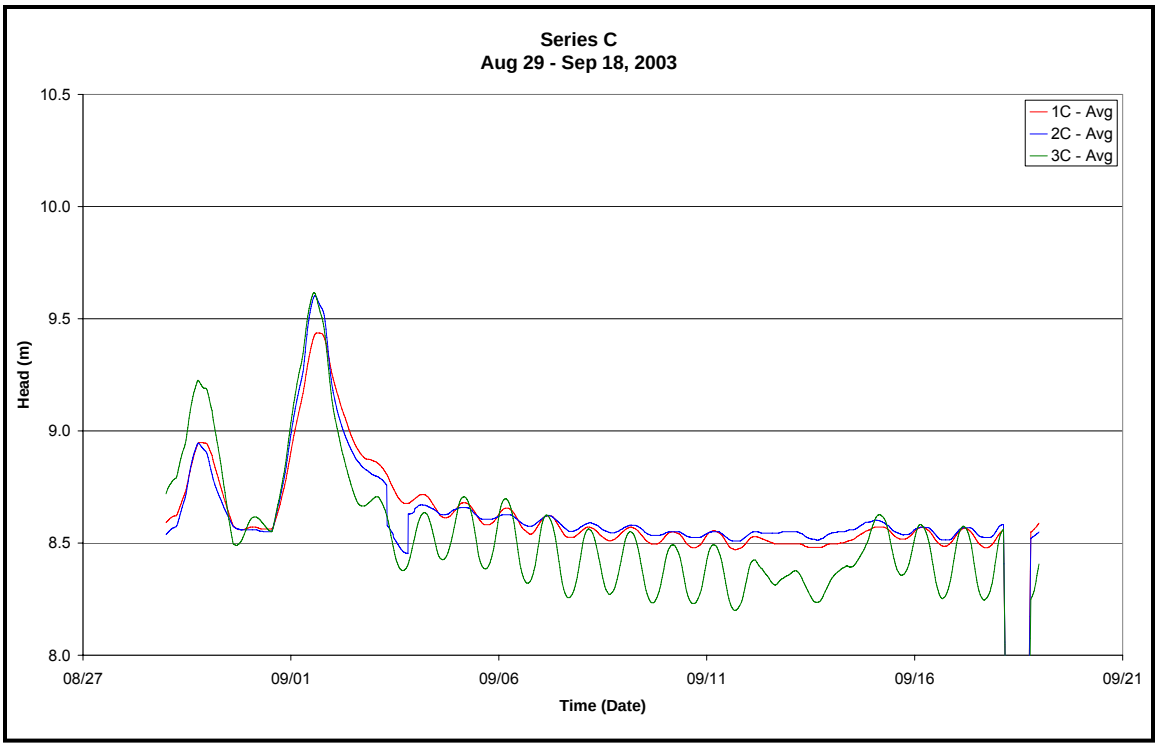

Figure 16: Series C piezometers logged head measurements, August 29-September 18,

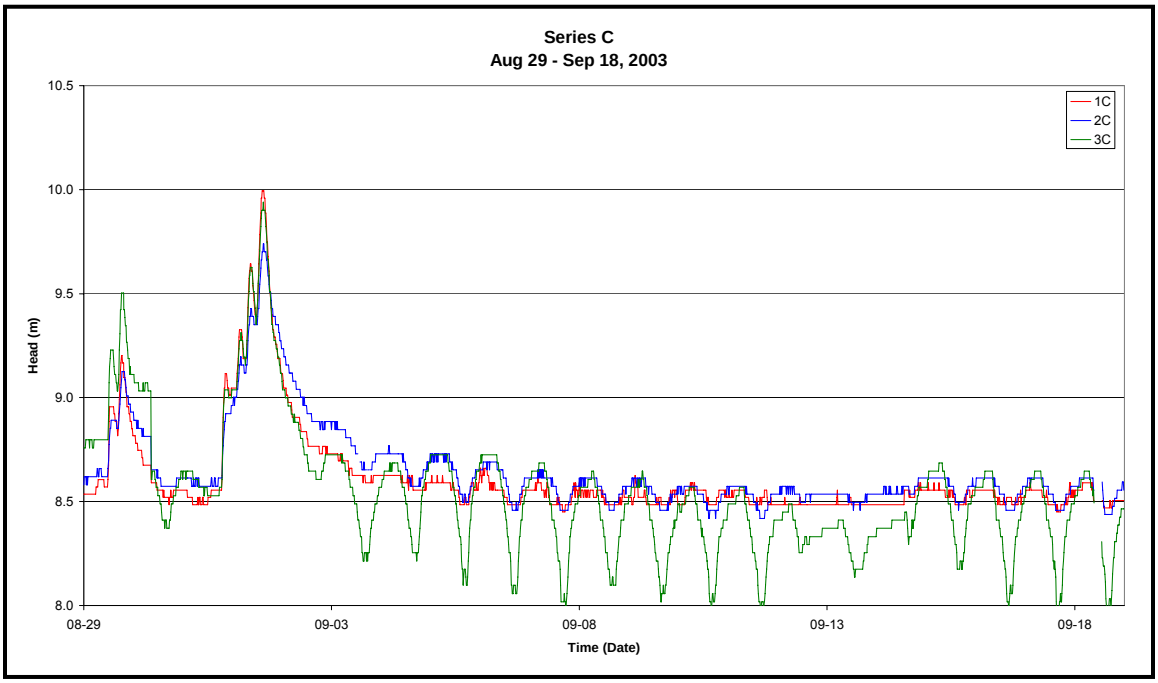

Figure 17: Series C piezometers logged head measurements, August 29-September 18,

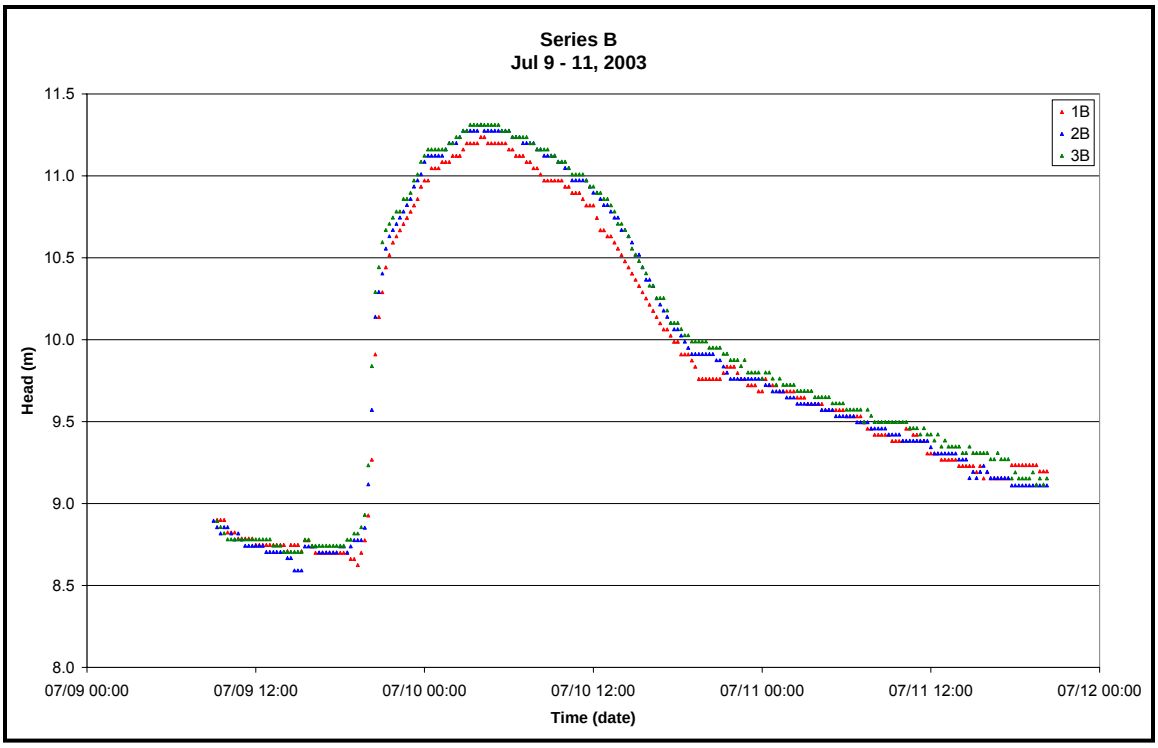

Figure 18: Series B piezometers logged head measurements, July 9-11, 2003.

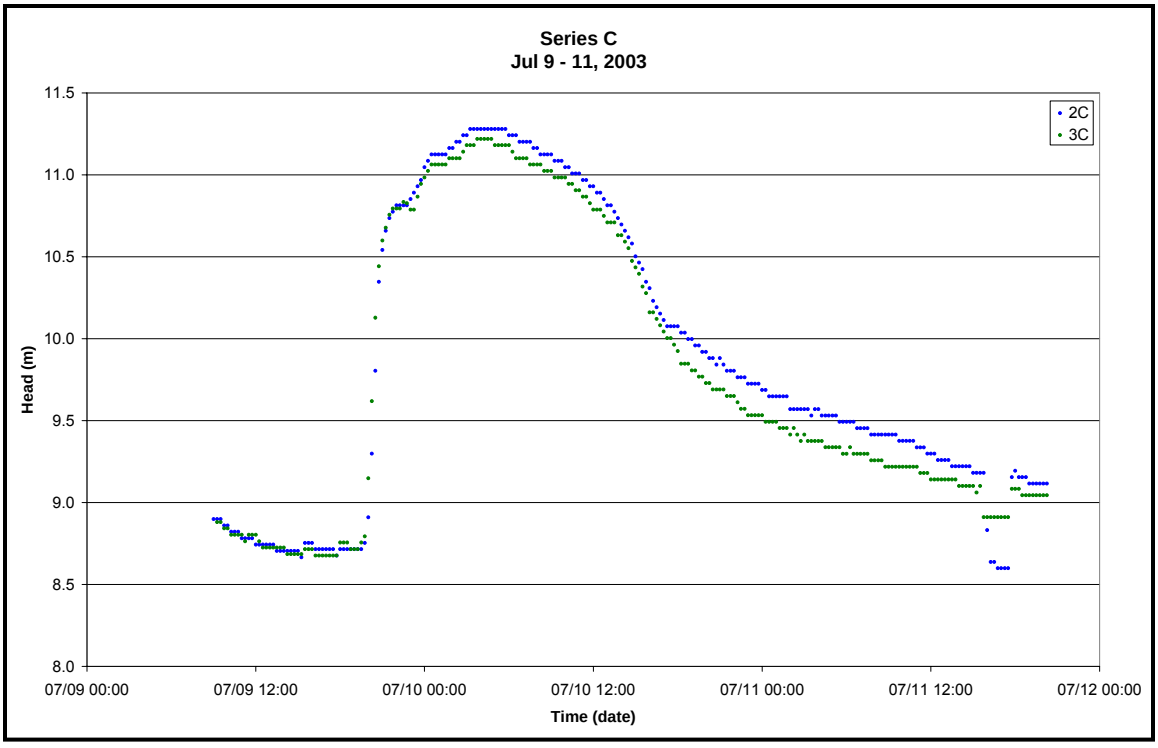

Figure 19: Series C piezometers logged head measurements, July 9-11, 2003.

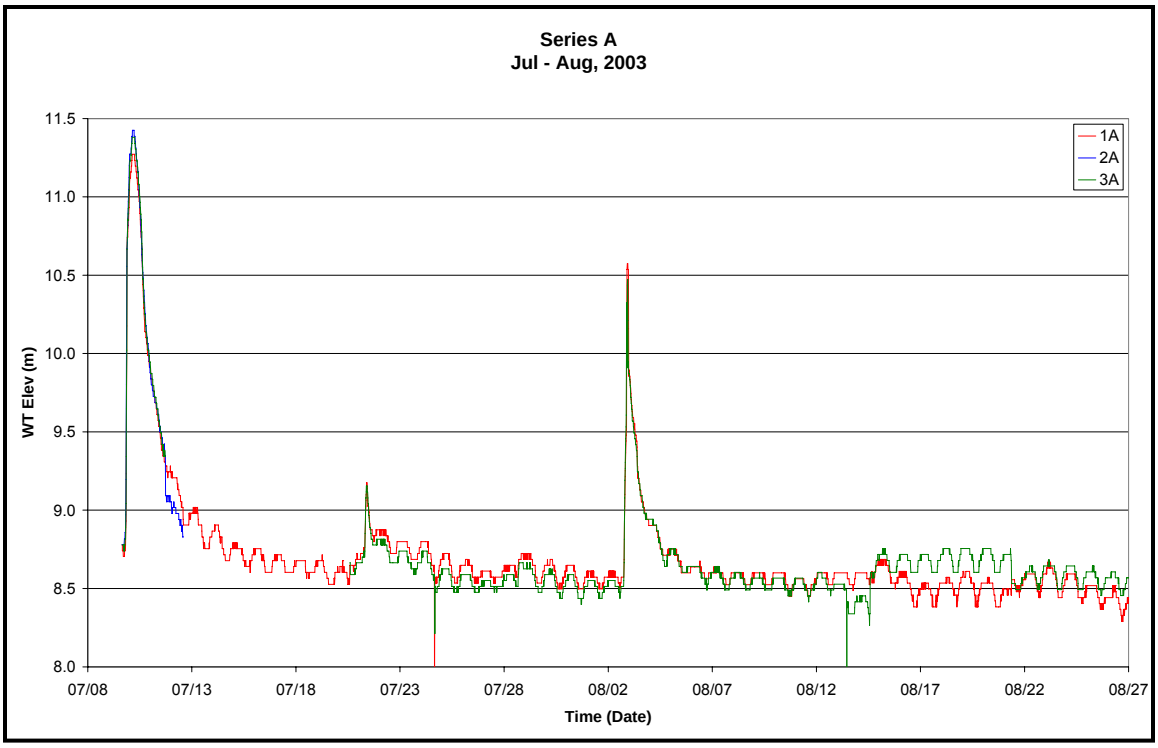

Figure 20: Series A piezometers logged head measurements, July-August, 2003.

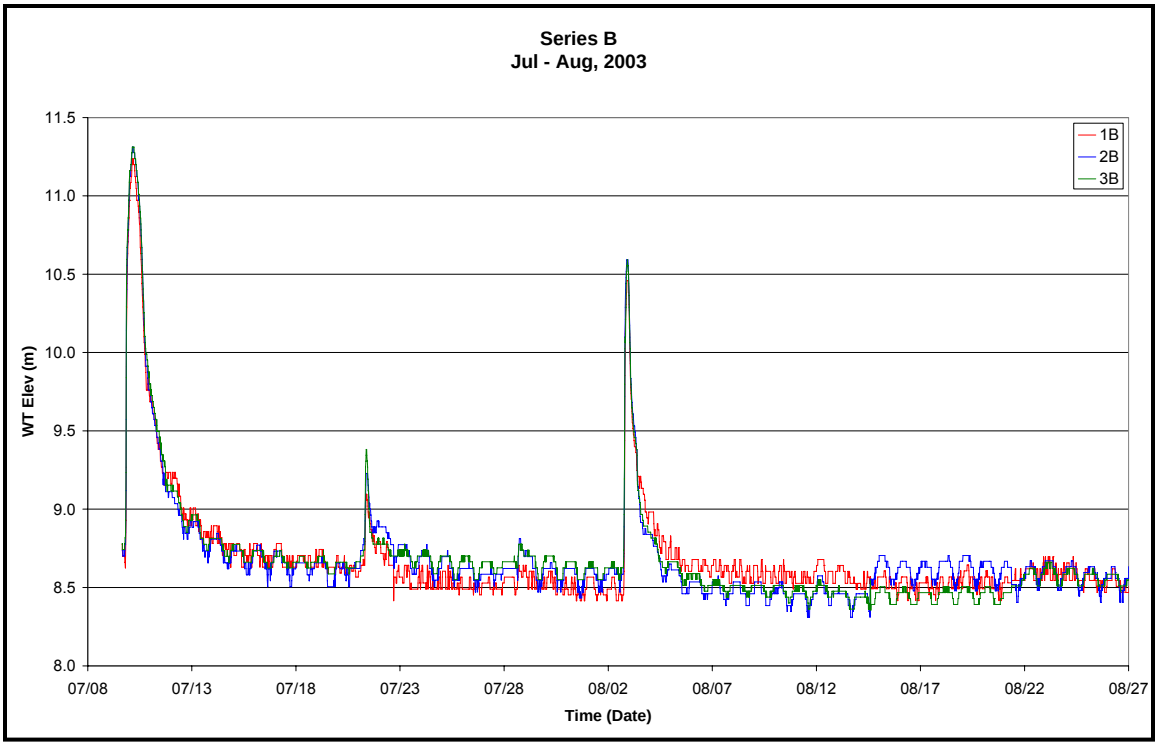

Figure 21: Series B piezometers logged head measurements, July -August, 2003.

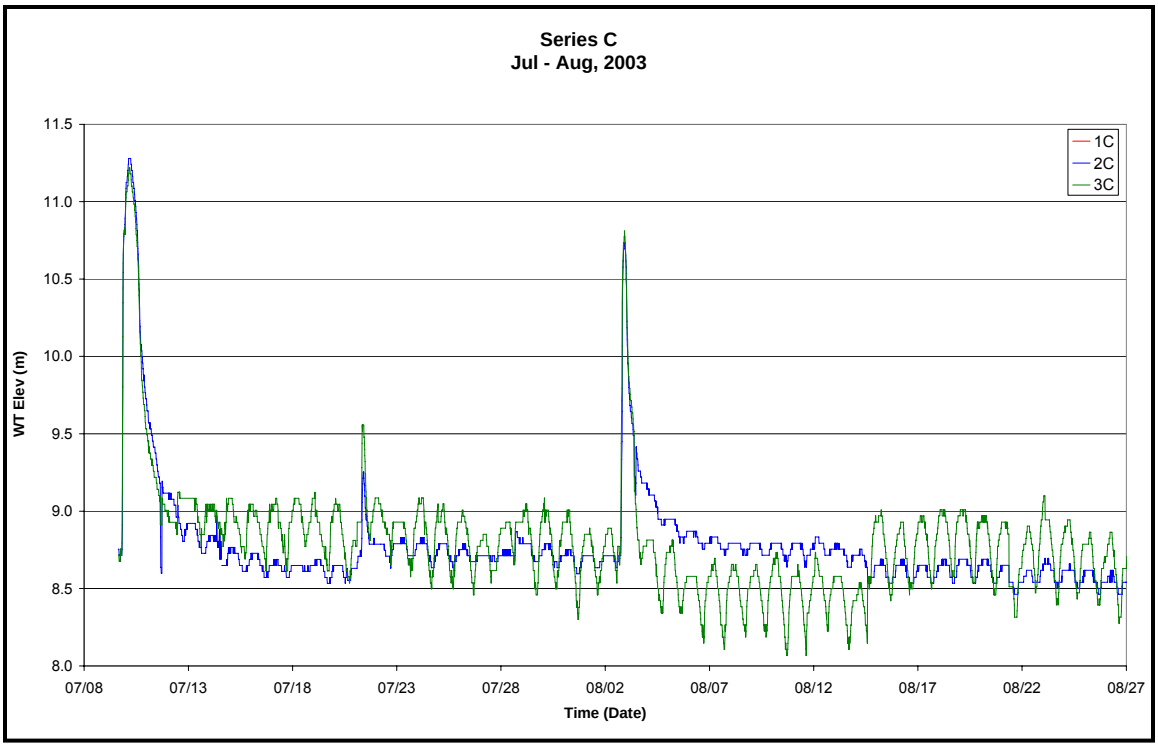

Figure 22: Series C piezometers logged head measurements, July-August, 2003.

CHAPTER III

ESTIMATING *K* BY CALIBRATING A 1D TRANSIENT MODEL

Hypothesis/Null Hypothesis

Within dynamic porous media systems, pressure variations over space propagate over time as a function of the hydraulic conductivity, *K*, of the medium (Silin et al. 2003). Measurements of the natural subsurface variations in *h* induced by variations in stream stage can be used as input to a one-dimensional model to estimate *K*. However, heterogeneities in the medium, temporal changes such as scour of and deposition onto the stream bed, and dynamic variations in the three-dimensional flow field may confound attempts to interpret *in situ* one-dimensional data.

Mathematics of the Model

Estimating *K* from stream head data requires solving a transient flow equation. Although the stream reach is a three-dimensional system, the close arrangement of the piezometers may allow us to simplify the model domain and describe the system in only the vertical dimension. The governing equation (Equation 8) is generally used to describe horizontal flow in a confined aquifer. In the case of an unconfined aquifer with vertical flow, the fundamental physics and mathematics remain unchanged but, rather than using storativity and transmissivity which include as a term the thickness of the aq-

$$\frac{\partial^2 h}{\partial z^2} = \frac{S_s}{K}\frac{\partial h}{\partial t} \tag{8}$$

$$h_i^{n+1} = 1/(((\Delta z^2 S)/(2K\Delta t)) + \alpha) * [\alpha(\widetilde{h}_i^{n+1}) + (\Delta z^2 S / 2K\Delta t) * h_i^n + (1-\alpha) * (\widetilde{h}_i^n - h_i^n))] \tag{9}$$

$$h_i^n : \text{head at node } i \text{ at timestep } n$$
$$\widetilde{h} = (h_{i-1}^n + h_{i+1}^n)/2 \tag{10}$$

i: node number
n: time step (stress period number)
Δz: distance between vertical nodes = 0.079 m
S: storage coefficient = 1
α: coefficient of implicit = 0.5
K: hydraulic conductivity
Δt: duration of time step = 900 s

uifer, we must revert to specific yield (S_y) and K. S_y,—the volume of water produced per volume of aquifer per decline in head—in the shallow subsurface with free water above the bed will be unity. This is a necessary consequence of the definition of the system, in which any withdrawal of water from the subsurface is necessarily replaced with surface stream water. If allowed to equilibrate, a unit decline of head in the subsurface will require a unit decline in stream stage.

The model domain is defined as the column extending from the deepest, ***A***, to the shallowest, ***C***, piezometer, discretized into 21-equally sized elements. The lower and upper boundaries for this model are the varying head values recorded in piezometers ***A*** and ***C***, respectively. The flow equation is solved semi-implicitly, varying K to minimize the residual between simulated and observed values for the ***B*** piezometer. For each pair of observations made at 15-minute intervals, the Crank-Nicholson forwarding difference

approximation (Equation 2) was applied iteratively until the error was less than 2.5×10^{-3} m. *[Actually, 2.39e-3 m]*. Values ranging four orders of magnitude were automatically tested using Microsoft Excel's *Solver* function to find the minimum.

To check the significance of the solution described above, head values for the ***B*** piezometer was also calculated by linearly interpolation between ***A*** and ***C*** using Equation 10.

The residuals at each time point were calculated as the observed minus the simulated head value (r_s), and as the interpolated minus the simulated head value (r_i). The residuals were then squared and summed to indicate the goodness of fit. The sum of the squared residuals for simulated values (Σr_s^2) were compared to the sum of the squared residuals for interpolated values (Σr^2). A simulation is considered potentially good when Σr_s^2 is less than Σr_i^2.

Sensitivity to K was tested for each simulation by varying K at least one order of magnitude greater and less than the minimum value determined by the simulation. The Σr_s^2 was plotted against K and visually examined to insure that the K value produces a minimum residual.

Implementation and Results of the Model

The stream subsurface is part of the larger, dynamic, integrated stream and ground water system and thus is subject to variations outside the scope of this model, including the effects of transient weather systems, insolation, and evapotranspiration. To avoid these complications, data for periods that exhibited a consistent pattern over a

period of at least six hours were selected. In general, recession limbs following relatively large precipitation events created the most appropriate patterns; rising limbs were also analyzed. The data collected over the six-month period from May through November 2004 provided six events suitable and useful for modeling, and during which data were successfully collected. Simulations of two events were successful and four were not. The method was applied to data from rising and falling stages. Simulated head at piezometer ***B*** closely matched observed head during two falling-stage periods. Simulated head for a third falling-stage period did not closely match observed heads, and approached values calculated by linear interpolation as the simulation became insensitive to changes in K. The two satisfactory models and the representative unsuccessful model are reported here.

Test 1: On 2003 August 3, head in ***LK3A*** decreased 0.23 m, head in ***LK3B*** decreased 0.26 m, and head in ***LK3C*** decreased 0.47 m over 7.25 hours. Head values for ***LK3B*** remained between values for ***LK3A*** and ***LK3C*** for all but one of thirty readings. Head values in all piezometers decreased regularly and smoothly. Simulated head values for ***LK3B*** are a good fit with observed values when $K = 2.7\times10^{-5}$ m/s. Linearly interpolated head values follow the trend of both the simulated and the observed values, but the simulated values are a better match: Σr_i^2 exceeds Σr_s^2 by a factor of 9.7. The plot of r^2 versus K shows that r^2 is at a minimum for the calibrated value of K.

Test 2: On 2003 October 19, head in ***LK2A*** varied by about 0.15 m with a net decrease of about 0.05 m, head in ***LK2B*** varied by about 0.10 m with no net change, and head in ***LK2C*** varied by about 0.10 m with a net decrease of about 0.10 m over 35.5

hours. Head values for ***LK2B*** were between the values of ***LK2A*** and ***LK2C*** for 36 of 143 readings. Simulated values only generally follow the overall trend; interpolated values appear to more closely track observed head values, but Σr_i^2 exceeds Σr_s^2 by a factor of 1.5. The plot of r^2 versus K shows a sharply defined minimum when $K = 1.6\times10^{-6}$ m/s.

Test 3: On 2003 August 29, head in ***LK3A*** decreased 0.19 m, head in ***LK3B*** decreased 0.38 m, and head in ***LK3C*** decreased 0.43 m over 7.25 hours. Head values for ***LK3B*** were between values of ***LK3A*** and ***LK3C*** for four of forty-three readings. Head values in all piezometers decreased, but ***LK3B*** decreased most rapidly and became less than both ***LK3A*** and ***LK3C***. Both simulated and interpolated head values for ***2B*** follow the trend of observed values, but neither set is a good fit: Σr_s^2 exceeds Σr_i^2 by a factor of 1.03 when $K = 8.4\times10^{-4}$ m/s, and the simulation values alternate closely above and below the linear interpolation values. The plot of r^2 versus K shows that r^2 reaches a minimum when $K = 8.4\times10^{-4}$ m/s.

Test 4: During a rising stage on 2003 August 29, head in ***LK2A*** increased 0.38 m, head in ***LK2B*** increased 0.49 m, and head in ***LK2C*** increased 0.50 m over 8.5 hours. Head values for ***LK2B*** were higher than for either ***LK2A*** or ***LK2C*** for twenty-three of the thirty-five readings Both simulated and interpolated head values for ***2B*** closely follow the trend of observed values, but neither set is a good fit: Σr_s^2 exceeds Σr_i^2 by a factor of 1.23 when $K = 1\times10^{\square 3}$ m/s. The plot of r^2 versus K shows that r^2 does not reach a minimum.

Test 5: During the falling limb on 2003 Aug 29, head in ***LK2A*** decreased 0.30 m, head in ***LK2B*** decreased 0.38 m, and head in ***LK2C*** decreased 0.27 m over 10.5 hours. Head values for ***LK2B*** remained between values of ***LK2A*** and ***LK2C*** for all but five of forty-three readings. Head values in all piezometers decreased regularly and smoothly, but ***LK2B*** values decreased faster than the other two. Both simulated and interpolated head values for ***2B*** follow the trend of observed values, but neither set is a good fit: Σr_s^2 exceeds Σr_i^2 by a factor of 1.1 when $K = 4\times10^{-4}$ m/s. The plot of r^2 versus K shows that r^2 does not reach a minimum.

Test 6: On 2003 November 18 through November 20, head in ***LK2A***, fell by about 0.9 m while ***LK2B***, and ***LK2C*** each fell by about 1.1 m over 48.25 hours. Values for ***LK2B*** fell between the values for ***LK2A*** and ***LK2C*** for 94 of the 194 observations. Head readings in all piezometers decreased regularly and smoothly. Both simulated and interpolated head values for ***LK2B*** closely follow and match observed values, but interpolated values are marginally closer than simulated values: Σr_s^2 exceeds Σr_i^2 by a factor of 1.03. The plot of r^2 versus K shows no minimum.

Other Estimates of *K*

One sample of the stream bed material was collected from within five meters of the study site, and two samples were collected several hundred meters downstream. The samples were collected by driving three-inch inside diameter pipe into the sediment until refusal, applying a vacuum, and levering or jacking out the pipe. Sediment recovery ranged from none to nearly intact. Recovered sediment was analyzed by sieve and pi-

pette. The sample collected near the study site is about 70% fine to medium sand or larger ($\varphi \leq 1.4$) with about 10% very fine sand or smaller ($\varphi \geq 2.5$). *K* was estimated using the Hazen equation, giving a value of about 4×10^{-4} m/s. The samples collected downstream are about 70% coarse sand or larger ($\varphi \leq 0$) with less than 5% silt and clay ($\varphi \geq 5$). Hazen-method estimates of *K* ranged from 10^{-3} to 10^{-1} m/s.

Previous analysis of similar material has yielded average values for *K* ranging from a low value of 10^{-7} m/s for silty sand to a high value of 10^{-2} m/s for clean sand (Freeze and Cherry, 1979).

Analysis and Discussion

Test 1 in nest ***LK3*** using data collected while the stream stage was falling on August 3 provided a good data set for the model, with a minimum r^2 when *K* is equal to $2.7´10^{-5}$ m/s, a well-defined minimum r^2 value, and a realistic estimate of *K*. Test 2 in nest ***LK2*** using data collected during base flow on October 19 yielded a simulation residual significantly lower than the interpolation residual, a sharply defined minimum residual, and a realistic estimate of *K* equal to $1.6´10^{-6}$ m/s. The two estimates differ by a factor of about 17, or 1.2 orders of magnitude. The estimates of *K* are reasonable and within published averages for unconsolidated silty to clean sand. The results of these two simulations suggest that calibration of a one-dimensional transient model can occasionally produce realistic estimates of *K* in a shallow stream subsurface. The estimate of $K = 4\times10^{-4}$ m/s from a nearby sample using the Hazen method is about one to two orders of magnitude greater than the simulation estimate. The Hazen and most other methods

were developed to estimate *K* in the horizontal plane as a tool for evaluating aquifer potential. Even relatively homogenous sediments are bedded to some degree, creating anisotropy that reduces vertical *K* by about an order of magnitude. Thus, the Hazen estimate of *K* is consistent with the simulation estimate. However, the results from Test 2 are ambiguous: the *K*-estimate is reasonable, the simulation curve is smooth, and the plot of residuals shows a sharp minimum; but the input data appears chaotic and the apparently good results may be fortuitous. A statistically significant number of simulations using similar base flow data would have to be run to determine if this result is significant.

The remaining four tests, Test 3 through Test 6, illustrate other difficulties in applying this technique of model calibration. In Tests 3 and 4, the ***B***-series head values most frequently are not between ***A*** and ***C***; the simulation can only predict the value of the ***B***-series head values when it is between the bounding values. In both cases, the simulated head values closely track linear interpolation values. In Test 3, the simulated values become increasingly unstable as *K* increases. The *K* values of 8.4×10^{-4} m/s and $1´10^{-3}$ m/s for Test 3 and Test 4, respectively, are about the same as the value estimated by the Hazen method, and about one order of magnitude greater than the estimate from Test 1 and two orders of magnitude greater than the estimate from Test 2. Test 5 shows that when the observed values for ***LK2B*** changes faster than the bounding values of ***LK2A*** and ***LK2C***, the simulation cannot predict ***LK2B*** values. Test 6 illustrates that there must be a sizable difference in ***A***-, ***B***-, and ***C***-series observations for the model to produce significant results.

The two apparently successful simulations, Test 1 and Test 2, minimized the residual when K was on the order of 10^{-5} m/s; the remaining simulations predicted head values approaching the value predicted by linear interpolation when K was on the order of 10^{-4} to 10^{-3} m/s. Inspection of Equation 2 shows that as K increases, the equation reduces to linear interpolation.

The inconsistent results produced by these simulations strongly suggest either an incomplete conceptual model of the system, inadequate resolution in space and time to describe the propagation of head, or both. These tests may show limitations of the one-dimensional conceptual domain, further complicated by the piezometers being arranged over a horizontal length of about 1 m. Addressing this issue will require either a more complex two- or three-dimensional model, integration of the piezometers into a single bundle, or both.

Conclusion

This study shows that a perennial stream occasionally creates the dynamics—the changes in head over time between the shallow and deeper subsurface—to provide input for a transient model that can be calibrated to estimate vertical hydraulic conductivity of the streambed. However, because the method requires multiple instruments and works best during long falling recession limbs, it may not be practical or economical unless the instruments have been installed as part of a larger, longer term study. Within the studied glacial plain environment, only two events were successfully simulated over the six-

month period. It may be possible to overcome these limitations by bundling the instruments into a multi-level piezometer and by using higher-resolution instruments.

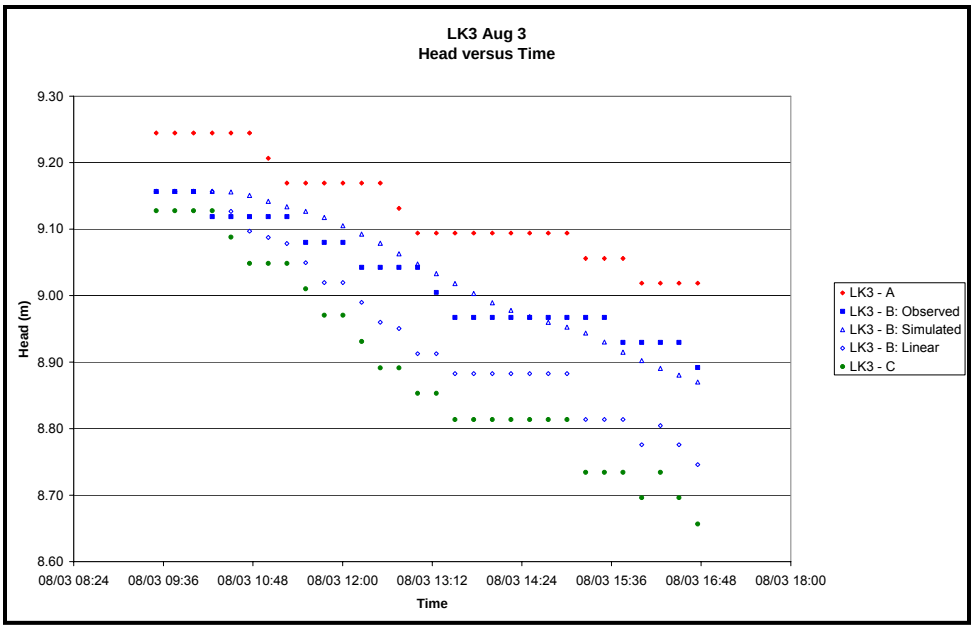

Figure 3.1: Observed and simulated head values for *LK3*, 2003 August 3.

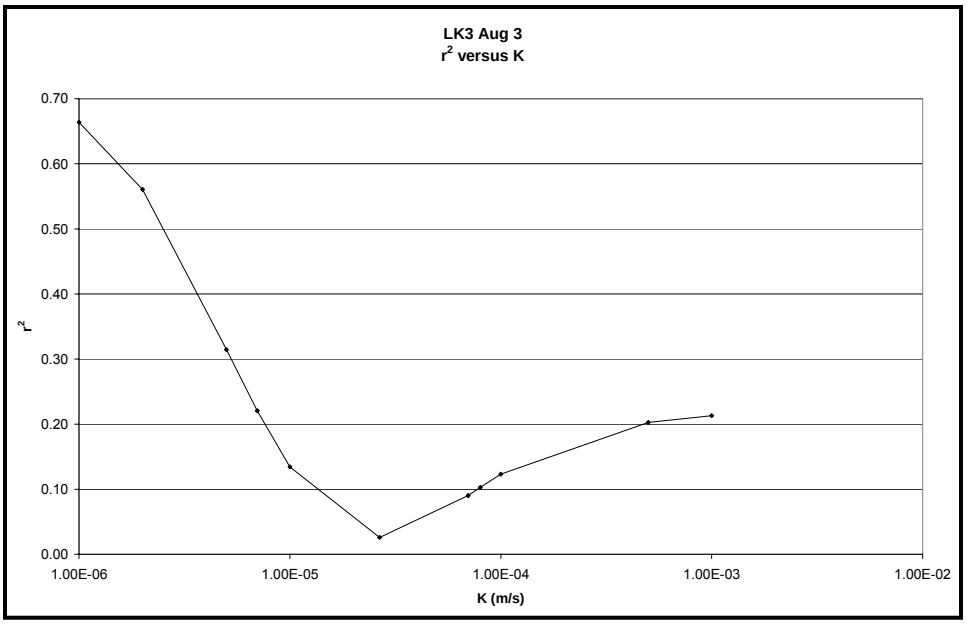

Figure 3.2: Squared residual as a function of *K* for *LK3*, 2003 August 3.

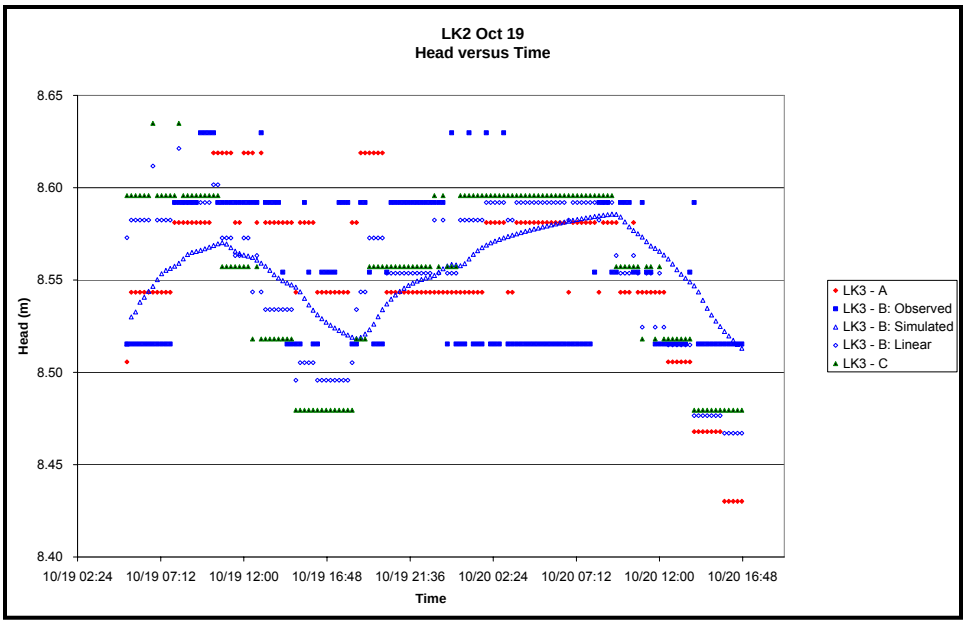

Figure 3.3: Observed and simulated head values for *LK2*, 2003 October 19.

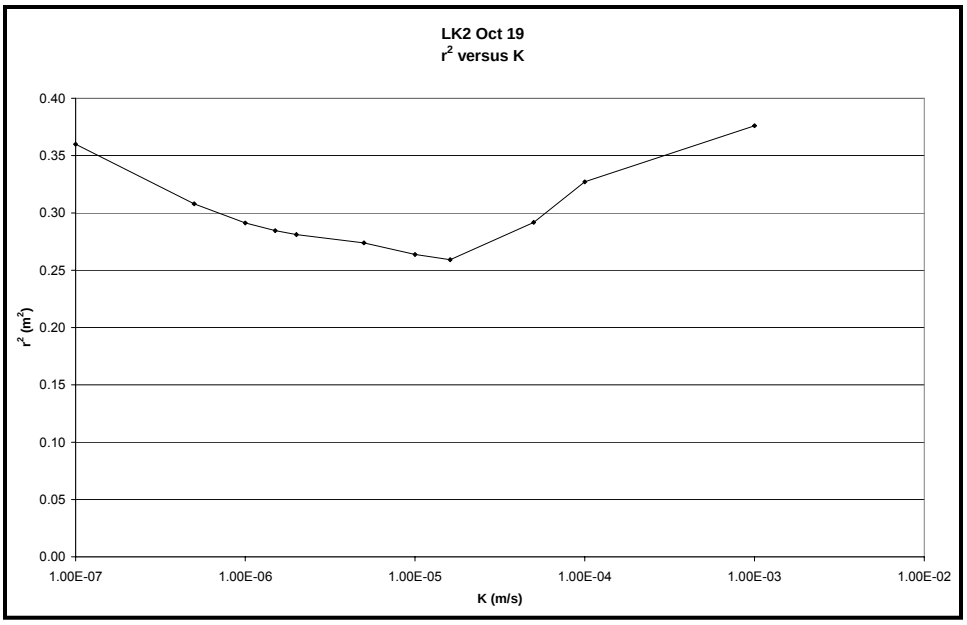

Figure 3.4: Squared residual as a function of *K* for *LK2,* 2003 October 19.

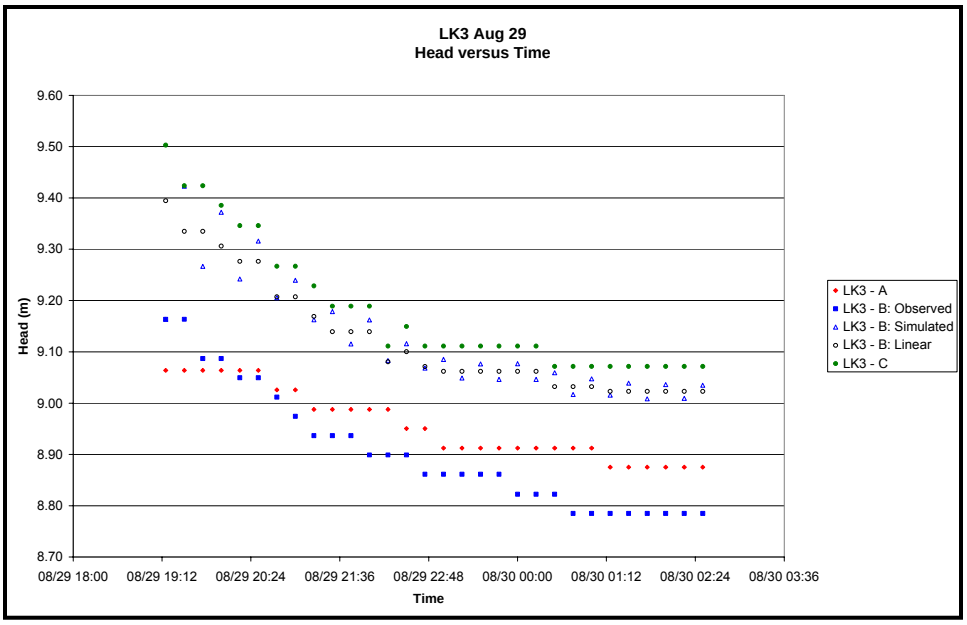

Figure 3.5: Observed and simulated head values for *LK3*, 2003 August 29.

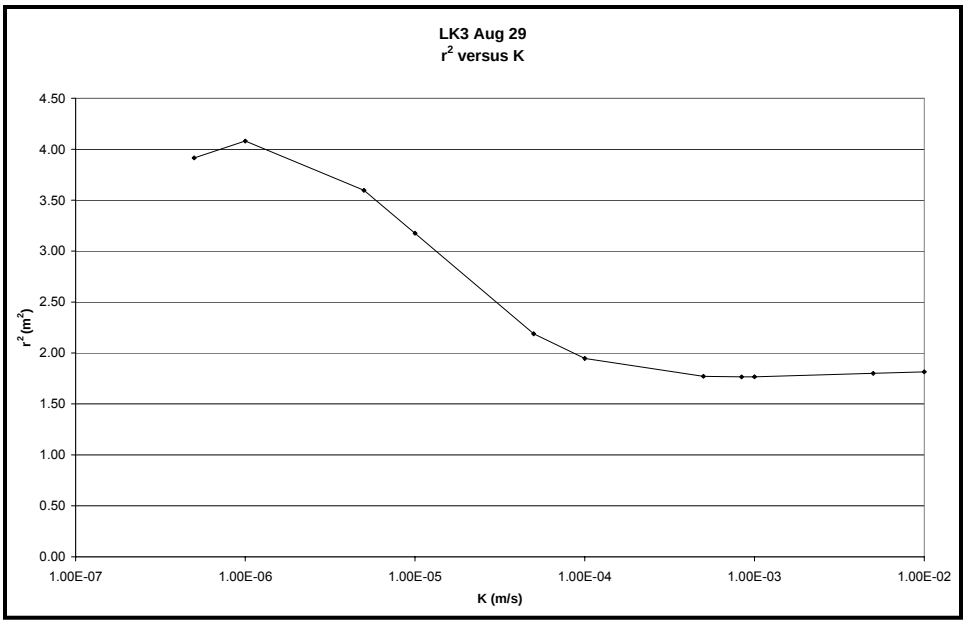

Figure 3.6: Squared residual as a function of *K* for *LK3*, 2003 August 29.

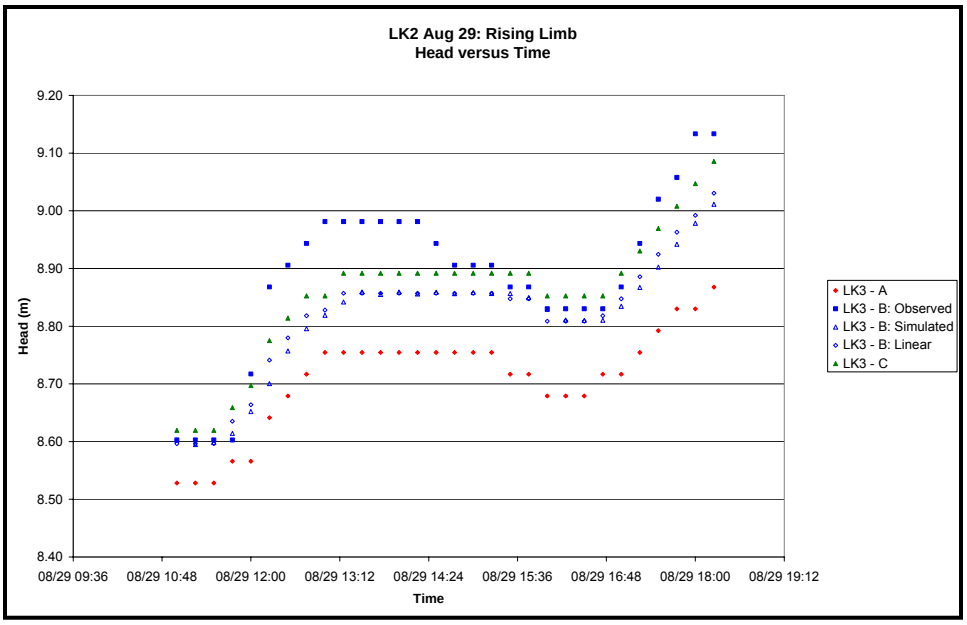

Figure 3.7: Observed and simulated head values for *LK2*, rising limb, 2003 August 29.

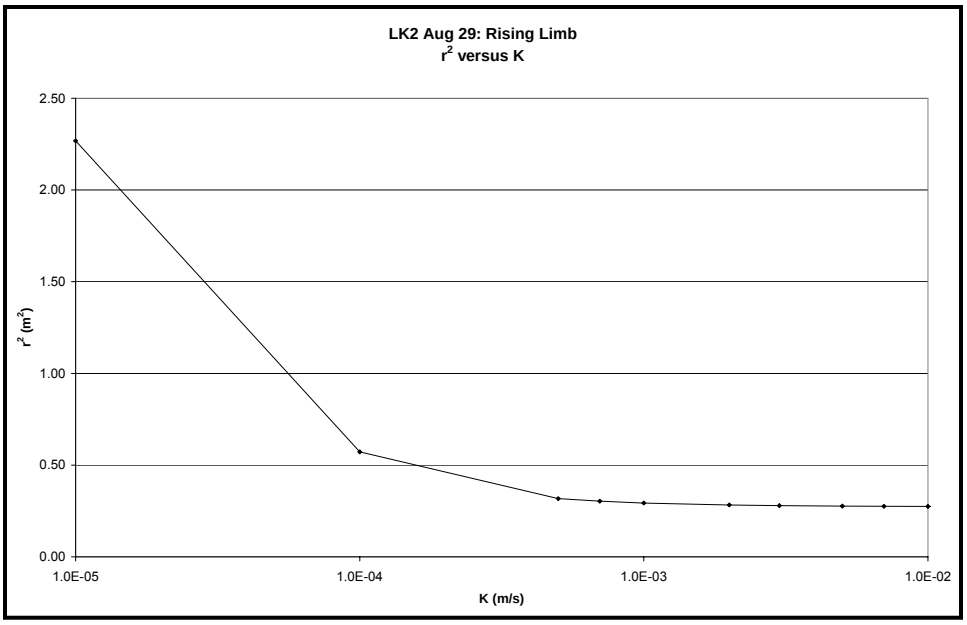

Figure 3.8: Squared residual as a function of *K* for *LK2*, rising limb, 2003 August 29.

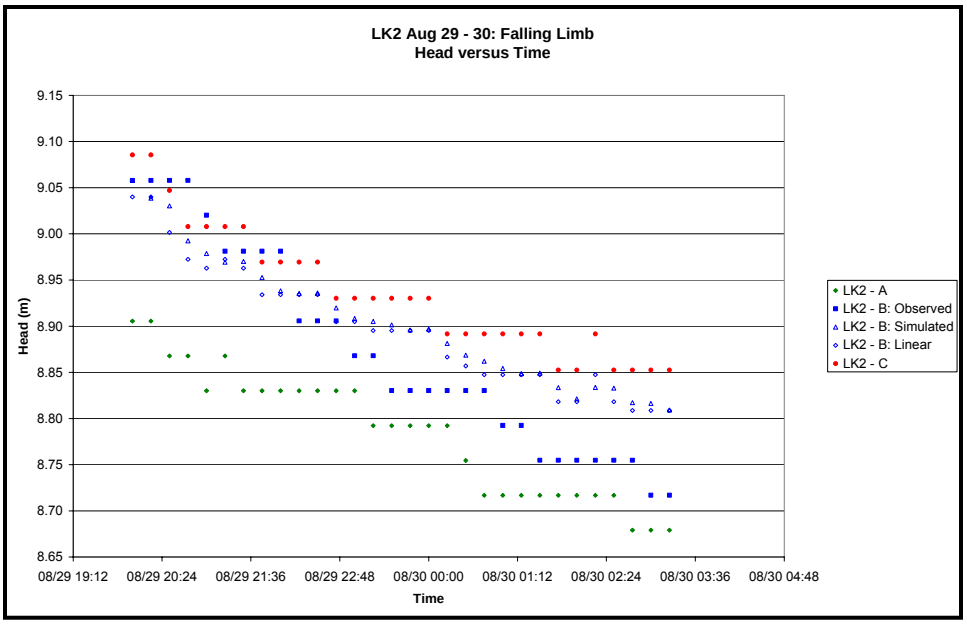

Figure 3.9: Observed and simulated head values for *LK2*, recession limb, 2003 August 29.

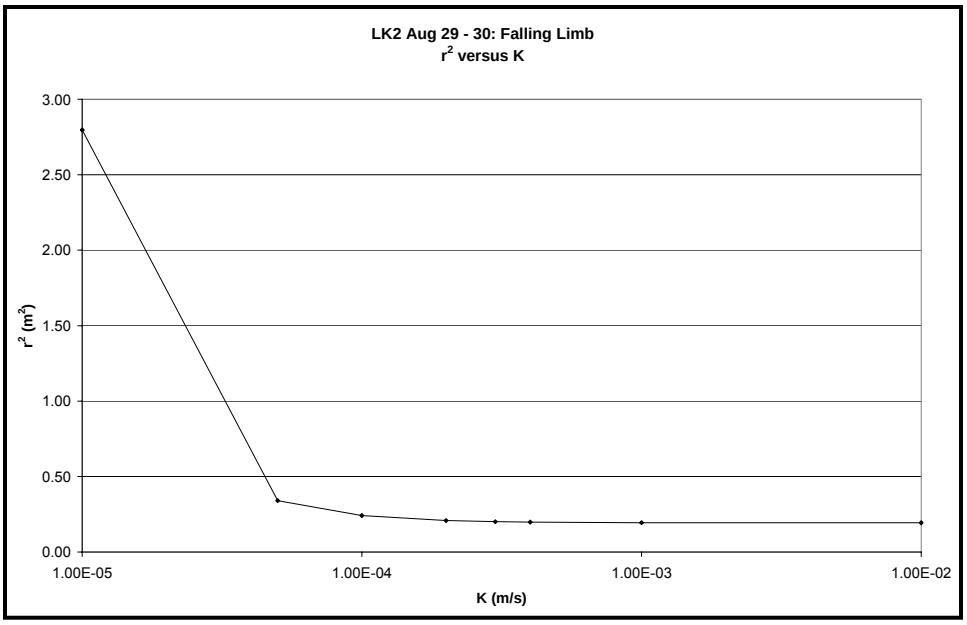

Figure 3.10: Squared residual as a function of *K* for *LK2*, recession limb, 2003 August 29.

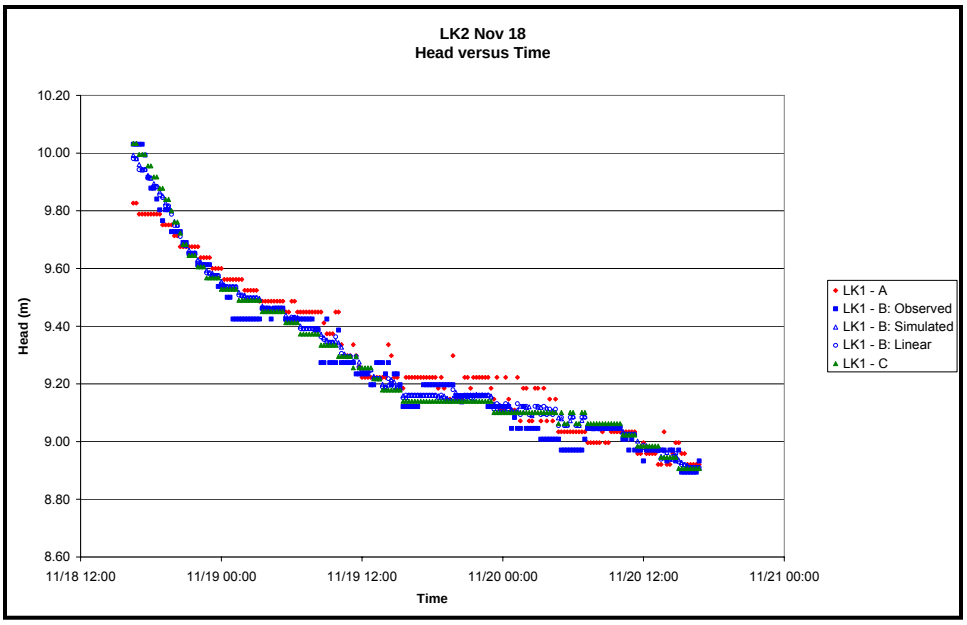

Figure 3.11: Observed and simulated head values for *LK2*, 2003 November 18-20. .

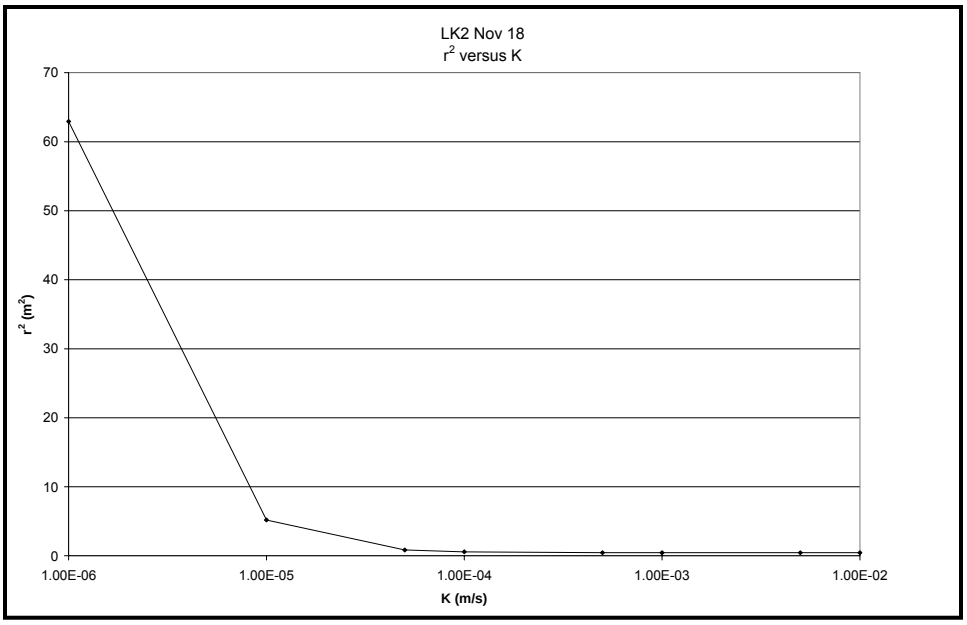

Figure 3.12: Squared residual as a function of *K* for *LK2*, 2003 November 18-20.

SUMMARY

Attempts to use transient head data in this study's small-scale models do not yield useful results. Further study of the physics of the experimental system shows that the proposed—and tested—methods implicitly assume that head propagates through the system in a manner and rate similar to the propagation of mass; specifically, as described by Darcy's Law for the flow of fluid through a porous medium. As Bernoulli's equation states, head is a form of energy. The stream and subsurface experimental system does conserve energy on the large scale, and transmit energy through the small scale, but it does so at a rate that cannot be measured practically at the scale of this study. If pressure (*head*) propagates, for example, at the same rate as the dilational-contractional seismic P-waves, then propagation occurs on the order of 10^3 m/s. This, however, is demonstrably not correct. Recent studies of confined sand-and-gravel aquifer systems (Willems 2004, McGarry 2004 in preparation, Peterson and Sickbert 2004 in preparation) show head propagating at a rate on the order of a meter per second over ranges from meters to kilometers.

Conceptually, the physical methods described in these studies may be useful if it can be demonstrated that pressure propagates through the medium at a practically measurable rate. The hyporheic zone plays a critical role in stream and riparian ecosystems, and understanding the physical controls on water exchange between the surface and the

subsurface is necessary to characterize the dynamics of the system. The questions addressed here warrant further study, but will require a conceptual model based not on Darcy's Law, but on fundamental fluid dynamics.

The rate of propagation of head may also affect attempts to detect and quantify the Venturi Effect through head measurements in the field. Previous laboratory studies have used visible tracers to demonstrate the effect of small pressure variations created by stream bedforms (Thibodeaux and Boyle, 1987). Visible tracer experiments might be of limited utility when looking for effects caused by lateral velocity differences because it is more difficult to set up visible access to a cross-section normal to flow than along flow. Therefore, future research will require either an entirely different method, or use the method of this study with higher resolution.

The rate of propagation of head, in any case, will be too great to allow demonstration or measurement of the Venturi Effect.

REFERENCES

Boulton, Andrew J., Stuart Findlay, Pierre Marmonier, Emily H. Stanley, and H. Marice Valett. 1998. The functional significance of the hyporheic zone in streams and rivers. *Annual Review of Ecological Systems* 9: 59-81.

Bouwer, J., and R. C. Rice. 1976. A slug test for determining hydraulic conductivity of unconfined aquifers with completely or partially penetrating wells. *Water Resources Research*, 12 no. 3: 423-428.

Cutnell, J. D., and K. W. Johnson. 2001. *Physics*, 5th ed. New York: John Wiley & Sons.

Domenico, P.A., and F.W. Schwartz. 1990. *Physical and Chemical Hydrogeology*, 2nd ed. New York: John Wiley and Sons.

Duff, J.H., F. Murphy, C. C. Fuller, F. J. Triska, J. W. Harvey, and A. P. Jackman. 1998. A mini drive point sampler for measuring pore water solute concentrations in the hyporheic zone of sand-bottom streams. *Limnology and Oceanography* 43 no. 6: 1378-1383.

Duff, J.H., B. Toner, A. P. Jackman, and F. J. Triska. 2000. Determination of groundwater discharge into a sand and gravel bottom river: a preliminary comparison of chloride dilution and seepage meter techniques. *Internationale Verieinigung fur Theoretische und Angewandte Limnologie, Vernhandlungen* 27: 1-6.

Elliott, A. H., and N. H. Brooks. 1997a. Transfer of nonsorbing solutes to a streambed with bed froms; Theory. *Water Resources Research* 33 no. 1: 123-136.

Elliott, A. H., and N. H. Brooks. 1997b. Transfer of nonsorbing solutes to a streambed with bed forms; laboratory experiments: *Water Resources Research* 33 no. 1: 137-151.

Hakenkamp, C. C., H. M. Valett, and A. J. Boulton. 1993. Perspectives on the hyporheic zone: integrating hydrology and biology, concluding remarks. *Journal of the North American Benthological Society* 12 no. 1: 94-99.

Harvey, J. W., and K. E. Bencala. 1993. The effect of streambed topography on surface-subsurface water exchange in mountain catchments. *Water Resources Research* 29 no. 1: 89-98.

62

Harvey, J. W., B. J. Wagner, K. E. Bencala. 1996. Evaluating the reliability of the stream tracer approach to characterize stream-subsurface water exchange. *Water Resources Research*, 32 no. 8: 2441-2451.

Harvey, J. W., and B. J. Wagner. 1999. Quantifying Hydrologic Interactions between Streams and Their Subsurface Hyporheic Zones. In *Streams and Ground Waters*, edited by J. B. Jones and P. J. Mulholland. San Diego: Academic Press.

Hinkle, S.R., J. H. Duff, F. J. Triska, A. Laenen, E. B. Gates, K. E. Bencala, D. A Wentz, and S. R. Silva. 2001. Linking hyporheic flow and nitrogen cycling near the Wilamette River - a large river in Oregon, USA. *Journal of Hydrology*, 244: 157-180.

Hvorslev, M. J. 1951. Time lag and soil permeability in ground water measurements. *Bulletin 36* Vickburg, MS: U. S. Army Corps of Engineers, Waterways Experimental Station.

Hynes, H. B. N. 1974. Further studies on the distribution of stream animals within the substratum. *Limnology and Oceanography*, 19: 92-99.

Illinois State Water Survey. 1995. Surface Water and Flood Plain Information Services. http://www.sws.uiuc.edu/fpi/cfd.asp?s=2&riverID=170&countyid=64. (June 13, 2005).

Larkin, R. G. and J. M. Sharp. 1992. On the relationship between river-basin geomorphology, aquifer hydraulics, and ground-water flow direction in alluvial aquifers. *Geological Society of America Bulletin*, 104: 1608-1620.

Libelo, E. L., and W. G. MacIntyre. 1994. Effects of surface-water movement on seepage-meter measurements of flow through the sediment-water interface. *Applied Hydrogeology*, 2: 49-54.

Mulholland, P. J., and D. L. DeAngelis. 1999. Surface-Subsurface Exchange and Nutrient Spiraling. In *Streams and Ground Waters*, edited by J. B. Jones and P. J. Mulholland. San Diego: Academic Press.

Neuman, S. P. 1975. Analysis of pumping test data from anisotropic unconfined aquifers considering delayed gravity response. *Water Resources Research*, 11: 329-342.

Packman, A. I., and Bencala, K. E. 1999. Modeling methods in the study of surface-subsurface hydrologic interactions. In *Streams and Ground Waters*, edited by J. B. Jones and P. J. Mulholland. San Diego: Academic Press.

Packman, A. I., N. H. Brooks, and J. J. Morgan. 2000. A physicochemical model for colloid exchange between a stream and a sand streambed with bed forms. *Water Resources Research* 36, no. 8: 2351-2361.

Packman, A. I., N. H. Brooks,, and J. J. Morgan. 2000. Kaolinite exchange between a stream and a streambed: Laboratory experiments and validation of a colloid transport model. *Water Resources Research* 36, no. 8: 2363-2372.

Palmer, M. A. 1993. Experimentation in the hyporheic zone: challenges and prospectus. *Journal of the North American Benthological Society* 12, no 1: 84-93.

Savant, S. A., D. D. Reible, and L. J. Thibodeaux. 1987. Convective transport within stable river sediments. *Water Resources Research* 23: 1763-1768.

Shanahan, P., D. Borchardt, M. Henze, W. Rauch, P. Reichert, L. Somlyódy, and P. Vanrolleghem. 2000. River Water Quality Model No. 1 (RWQM1): I. Modelling Approach. Paper presented at the 1st World Congress of the International Water Association (IWA), Paris, France, July 3-7, 2000.

D. Silin, V. Korneev and G. Goloshubin. 2003. Pressure diffusion waves in porous media. Paper presented at the 73rd SEG Meeting in Dallas, Texas.

Sophocleous, M. 2002. Interactions between groundwater and surface water: the state of the science. *Hydrogeology Journal* 10: 52-67.

Stanford, J. A., and J. V. Ward. 1993. An ecosystem perspective of alluvial rivers: connectivity and the hyporheic corridor. *Journal of the North American Benthological Society* 12, no. 1: 48-60.

Thibodeaux, L. J., and J. D. Boyle. 1987. Bedform-generated convective transport in bottom sediment. *Nature* 325: 341-343.

Triska, F.J., J. H. Duff, and R. J. Avanzino. 1993. Patterns of hydrological exchange and nutrient transformation in the hyporheic zone of a gravel bottom stream: Examining terrestrial aquatic linkages. *Freshwater Biology* 29: 259-274.

Triska, F. J., V. C. Kennedy, R. J. Avanzino, G. W. Zellweger, and K. E. Bencala. 1989. Retention and transport of nutrients in a third-order stream in northwestern California: Hyporheic Processes. *Ecology* 70, no. 6: 1893-1905.

United States Geological Survey. 1985. Bloomington East 7½' Topographic Quadrangle.

Valett, H. M., S. G. Fisher, N. B. Grimm, and P. Camill. 1994. Vertical hydrologic exchange and ecological stability of a desert stream ecosystem. *Ecology* 25, no. 2: 548-560.

White, D. S. 1993. Perspectives on defining and delineating hyporheic zones. *Journal of the North American Benthological Society* 12, no. 1: 61-69.

Ward, J. V. 1989. The four-dimensional nature of lotic ecosystems. *Journal of the North American Benthological Society* 8, no. 1: 2-8.

Ward, J. V. and J. A. Stanford. 1983. The intermediate-disturbance hypothesis: an explanation for biotic diversity patterns in lotic ecosystems. In *Dynamics of Lotic Ecosystems*. Edited by T. D. Fontain III and S. M. Bartell. Ann Arbor: Ann Arbor Science.

Ward, J. V., and J. A. Stanford, J. A. 1983. The serial discontinuity concept of lotic ecosystems. In *Dynamics of Lotic Ecosystems*. Edited by T. D. Fontain III and S. M. Bartell. Ann Arbor: Ann Arbor Science.

White, David S. 1993. Perspectives on defining and delineating hyporheic zones. *Journal of the North American Benthological Society* 12, no. 1: 61-69.

Willman, H. B. and J. C. Frye. 1970. Pleistocene Stratigraphy of Illinois, Bulletin 94. Urbana, IL: Illinois State Geological Survey.

Wörman, A., and A. I. Packman. 2002. Effect of flow-induced exchange in hyporheic zones on longitudinal transport of solutes in streams and rivers. *Water Resources Research* 38, no. 1: 1001.

Wroblicky, G. J., M. E. Campana, H. M. Valett, and C. N. Dahm. 1998. Seasonal variation in surface-subsurface water exchange and lateral hyporheic area of two stream-aquifer systems. *Water Resources Research* 34, no. 3: 317-328.